Mapping the Potential for Eolian Surface Activity in Grasslands of the High Plains using Landsat Images

by

Ethan Dain Gutmann

B.A., Williams College, 1999

A thesis submitted to the

Faculty of the Graduate School of the

University of Colorado in partial fulfillment

of the requirements for the degree of

Master of Science

Department of Geological Sciences

2002

Gutmann, Ethan Dain (M.Sc. Geological Sciences)

Mapping the Potential for Eolian Surface Activity in Grasslands of the High Plains using Landsat Images

Thesis directed by Professor Alexander F.H. Goetz

There are over 100,000 square kilometers of eolian sand dunes and sand sheets in the High Plains of the central United States. These land-forms may be unstable and may reactivate again as a result of land-use, climate change, or natural climatic variability. The main goal of this thesis was to develop a model that could be used to map an estimate of future dune activity. Multi-temporal calibrated Landsats 5 Thematic Mapper (TM) and 7 Enhanced Thematic Mapper Plus (ETM+) NDVI imagery were used in conjunction with the CENTURY vegetation model to correlate vegetation cover to climatic variability. This allows the creation of a predicted vegetation map which, combined with current wind and soil data, was used to create a potential sand transport map for range land in the High Plains under drought conditions.

This study found that Landsat is an excellent tool for mapping current dune activity, but the current model of sand transport does not allow for accurate predictions of future dune activity. Landsat spatial resolution is necessary to resolve small parabolic dunes of eastern Colorado, though MODIS scale imagery could be used in conjunction with Landsat data. This study shows that AVHRR scale data are far too coarse to use in studying dune activity. Landsat NDVI measurements, though imperfect, are readily able to distinguish different levels of vegetation cover present on dune crests vs interdune areas. Unfortunately, the available data were insufficient to generate a reasonable correlation between NDVI and CENTURY output. Further analysis showed that dividing the imagery into larger or smaller

regions did not significantly impact the quality of the regression, nor does the number of Landsat images, within the limited range of images available. This study was able to generate a reasonable map of current dune activity for range land areas across the High Plains and pointed out some of the problems inherent in attempting to predict future activity.

Acknowledgements

I would like to first and foremost thank my advisor Dr. Alexander Goetz for many years worth of discussions, comments, and guidance.

I would also like to thank the rest of my committee, Drs. Gifford Miller and Carol Wessman. Both of whom provided invaluable comments and suggestions.

Further thanks go to all of the people who have worked on this project or helped me at other times. Eric Johnson, Leanne Lestak, Kathy Heidebrecht, Bruce Kindel, Amanda Warner, Jen Mangan, Pete McIntosh, Peter Furey, Peter Gimeno, Valerie DeLoach, Tamara Palmer, Margaret Atkinson, Kathy Freeman, ... and many more.

Finally I would like to thank my parents, who have always encouraged my curiousity.

This research was supported by NASA grant NAGW5-3437.

Contents

Tables

Table

Figures

Figure

Chapter 1

Introduction

Extensive eolian sand deposits cover much of the High Plains of the United States. These deposits have been mobile at least four times in the past 10,000 years (Forman et al., 1992), and have the potential to remobilize in the future(Ahlbrandt et al., 1983; Muhs & Maat, 1993; Muhs et al., 1997). Today, these sand dunes and sand sheets are largely stabilized by vegetation (Muhs et al., 1996; Muhs & Holliday, 2001). Wind speeds are currently high enough that if vegetation were to be removed these dunes would likely remobilize. Vegetation in this area is highly susceptible to land use practices and periods of drought, such as the dust-bowls of the 1930s and 50s. During the 1930s and 50s, droughts, combined with poor land management practices, resulted in the reactivation of many of these sand deposits(Muhs & Maat, 1993). Because the High Plains are a major source of food production for the United States, future eolian activity could have important economic and social consequences. This project has attempted to map areas of instability in grasslands by combining regional climate data with Landsat 5 Thematic Mapper (TM) and Landsat 7 Enhanced Thematic Mapper Plus (ETM+) imagery.

This thesis is part of a large project studying the High Plains at the Center for the Study of Earth from Space (CSES). The long term goal of the project has been to map regions of instability and potential reactivation across the High

Plains. This larger project has collected three or more images from different years over each of thirty-three Landsat scenes in the High Plains and calibrated those scenes to apparent reflectance. During the course of the project regions of cloud free rangeland, as well as areas of pivot irrigation were hand digitized.

This project has taken a new approach towards the assessment of dune reactivation potential. Previous studies have focused on the history of the dune fields and regional climate (Forman et al., 2001; Woodhouse & Overpeck, 1998; Muhs et al., 1999; Muhs & Maat, 1993). Studies such as Woodhouse and Overpeck(1998) have examined the frequency of droughts and dune activity to determine what magnitude and duration of drought would be necessary to cause reactivation, as well as how likely such a drought is to occur under the current climate regime. These studies have been statistically based approaches to estimate the likelyhood of dune reactivation in a general sense. This study has taken a physically based approach to mapping locations that are likely to reactivate should such a drought occur. In the process I have tested the spatial resolution required for such a model, as well as the effect of temporal resolution. By combining a vegetation growth model (CENTURY), climate data, and Landsat Imagery into a single model, this project has generated a detailed map of potential dune reactivation for much of the High Plains.

A physically based model of dune reactivation has several advantages and disadvantages over previous studies. This model can readily incorporate estimations of future climate from GCMs. It also generates a map at the same scale as Landsat making it potentially useful for regional planning. However, this model is based on highly simplified models of the underlying processes and may not account for all of the necessary processes. Large-scale statistical studies of the types of climatic regimes which have existed in the past inherently account for all physical processes. These larger scale studies are only applicable to the future with

the assumption that processes will only change as they have historically. Because human land use has such a strong effect on the land surface, estimates of future dune activity that cannot account for human land use are flawed. Understanding the physical processes involved in dune reactivation is important when attempting to determine the probable state of the system in a variety of climate and land use scenarios.

Chapter 2

Background

2.1 High Plains

The High Plains extend from South Dakota to Texas, and cover portions of Colorado, Kansas, Nebraska, New Mexico, Oklahoma, and Wyoming (fig. 2.1). This area receives 200-900mm of rainfall per year, with much of it receiving less than 500mm. This classifies much of the area as semi-arid, and makes it highly susceptible to both human land use and climatic changes. Over 100,000 square kilometers are covered with aeolian sand dunes and sand sheets (fig. 2.1) (Madole, 1994) which have been active at least four times in the past 10,000 years (Forman et al., 1992), with large-scale activity in Nebraska and eastern Colorado occurring as recently as 260±60 ^{14}C yr. BP (Muhs et al., 1997) and evidence suggests wide spread activity in the 19th century as well (Muhs & Holliday, 1995). More recently, significant regional activity occurred during the dust-bowls of the early 20th century (Muhs & Maat, 1993). Because a large percentage of the food produced in the United States comes from this region, and many people live in this area, future changes in land cover are very important both socially and economically. In addition, paleo-dunefields are an important record of the regional climate over the past 10ky., thus a better understanding of the link between climate and dune activity may be helpful to paleoclimate studies.

In the High Plains, vegetation cover is the most important factor controlling

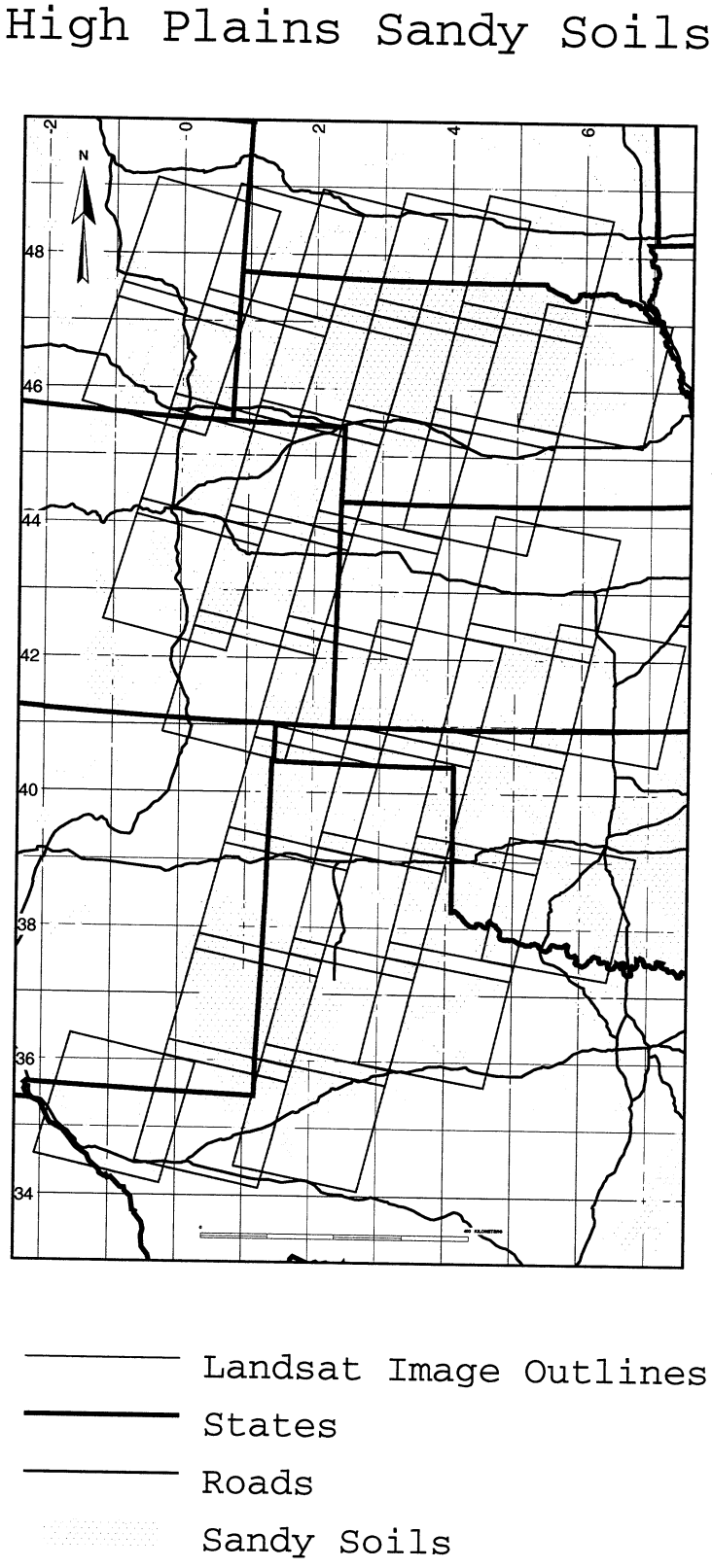

Figure 2.1: Sandy soils in the High Plains, based on the STATSGO database and Muhs and Holliday (1995). UTM Zone 14 projection, grid is in 100km intervals

sand activity. On partially vegetated sand surfaces, the amount of vegetation cover has been shown to be the dominant control on sand transport (Buckley, 1987; Wolfe & Nickling, 1993; Lancaster & Baas, 1998). Wind speeds in the High Plains are often well above the threshold velocity for sand transport, but vegetation cover prevents substantial sand movement. In addition the drift potential, a measure of the ability of wind in a region to transport sand (Fryberger & Dean, 1979), is intermediate to high for the central and northern High Plains (Muhs et al., 1996). In the southern High Plains Muhs and Holiday (2001) concluded that dunes are primarily stabilized by vegetation cover.

Studies have suggested that human induced climate change and natural climatic variability are likely to result in future droughts of the magnitude achieved in the early 1900s (Woodhouse & Overpeck, 1998). In addition, human land use effects the stability of land cover by influencing vegetation cover and surface cohesion. If overgrazing and heavy tilling become common practices, then large portions of the sand sheets will have a higher potential to reactivate again in the near future.

Sand dunes in the High Plains are highly susceptible to drought. Vegetation in the High Plains is largely water limited (Sala et al., 1988), thus, droughts are periods of high risk for sand activity. Aboveground net primary productivity (ANPP) in the High Plains is strongly correlated with precipitation, $R^2 = 0.9$ (Sala et al., 1988), and ANPP has varied by over ninety percent between wet and dry years in portions of the High Plains (Forman et al., 2001). In addition, periods of drought favor the expansion of shrubs over grasses (Schlesinger et al., 1989). Shrubs tend to be more spatially heterogeneous allowing greater erosion to occur in the interstices due to lack of cover and a funnelling effect that can locally increase the wind speed as air is forced to move around the shrubs.

The current level of dune activity typically increases from north to south.

Figure 2.2: This dune field north east of Kermit, Texas is highly active.

The most active dunes, such as those outside of Kermit, Texas (fig. 2.2), are located in Texas and New Mexico. Eastern Colorado contains large parabolic dunes, many of which have moderately active crests and frequent blowouts (fig. 2.3). The Nebraska sandhills make up the northern extent of this study. This area is characterized by large, currently stabilized, transverse dunes with occasional blowouts (fig. 2.4).

2.1.1 Previous Instances of Dune Reactivation

Sand dunes across the High Plains have been active numerous times in the past 10,000 years. Major dune activity is believed to have occurred in the mid Holocene, around 8-5 ^{14}C yr BP. Loope et. al (1995) and Stokes and Swinehart (1997) present evidence for activity in the Nebraska Sand Hills at this time. Forman and Maat (1990) and Forman et. al (1992; 1995) suggest that dune activity

Figure 2.3: Typical parabolic dunes in eastern Colorado. Largely stabilized by sparse vegetation cover, with a few blowouts. The fence is used to manage the extensive grazing in this region.

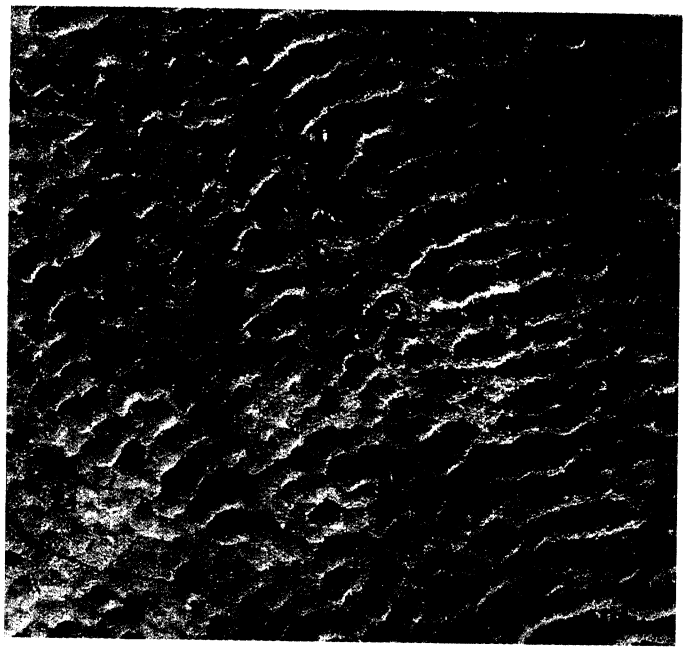

Figure 2.4: Landsat image of transverse dunes that cover much of central Nebraska. Most of this area is well stabilized, but on dune crests small blowouts still occur regularly. Across the region local ranchers work to limit natural blowouts from enlarging.

in eastern Colorado was also significant during periods of the mid-Holocene. In the southern High Plains, Holliday (1989; 1995) found evidence for mid-Holocene dune activity in dry valleys. More recently there have been numerous instances of eolian activity over much of the High Plains. Studies have shown the past 3,000 years to be a very active period across the High Plains (Muhs & Holliday, 1995; Forman et al., 1992; Loope et al., 1995; Muhs et al., 1996; Muhs et al., 1997; Stokes & Swinehart, 1997), the most recent of which probably occurred in the 19th century (Muhs & Holliday, 1995).

2.1.2 Effects of Land Use

Most of the High Plains are extensively impacted by human land use. Rangeland, used for grazing, and both irrigated and dryland farming are prominent through out the region. Some areas have been placed in the Conservation Reserve Program (CRP), a program that attempts to increase soil stability by paying farmers to plant natural grasses for ten year periods. This study does not look at areas which were farmed at any point during the period of study because vegetation in these areas responds more directly to variability in human activity then to variations in climate. Because most of the remaining grassland is grazed, it was impossible to avoid areas which have been impacted by land use patterns, but grazed areas are still likely to respond to weather forcings.

Grazing is a common use for land that is inhospitable to farming. Lands with substantial topography, such as sand dunes, or lands that do not have a source of water for irrigation and lack the nutrients necessary for productive dryland farming are often used primarily for cattle grazing. Variations in grazing can affect the vegetation cover substantially, thus weakening the correlation between climatic effects and vegetation cover. These effects are noticeable on individual Landsat scenes in which fence lines are prominent due to different grazing patterns

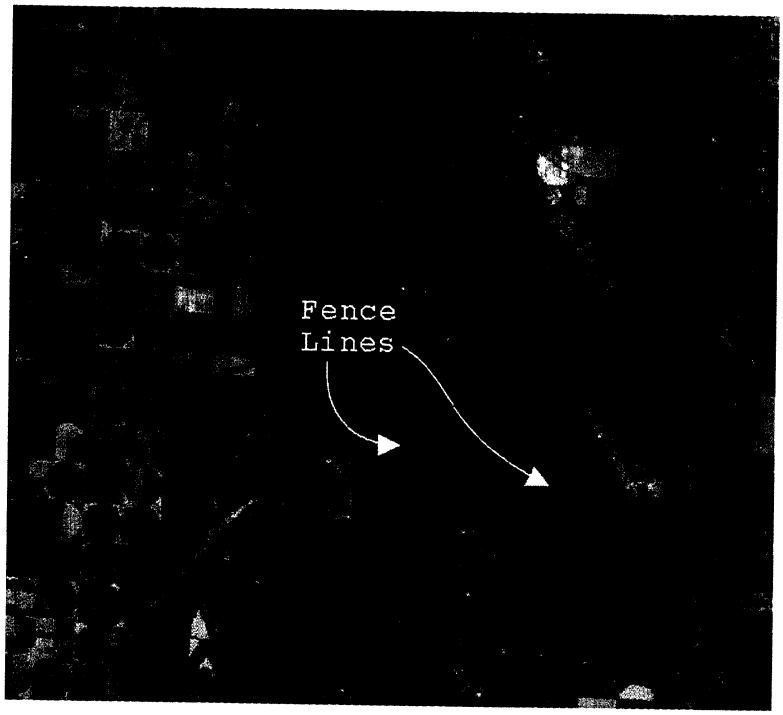

Figure 2.5: The effects of grazing on vegetation cover are visible in this CIR image from eastern Colorado. Hard lines between areas with different vegetation densities are indicative of recent variations in grazing patterns on opposite sides of a fence.

on opposite sides of the fence (fig. 2.5).

2.2 Potential Future Climate Change

Changes in the climate system could substantially affect the amount of moisture available for vegetation growth as well as wind speeds, and sediment availability in the High Plains (fig. 2.6). Under the current climate, moisture is primarily carried to the High Plains by upper level air masses from the Pacific Ocean and surface outflow from the Gulf of Mexico (Barry & Chorley, 1987) . Droughts are commonly associated with a weaker movement of air from the subtropical Atlantic and the Gulf of Mexico (Oglesby, 1991).

Much effort has been expended attempting to predict future climate. Many general circulation models indicate a general warming and drying over the High

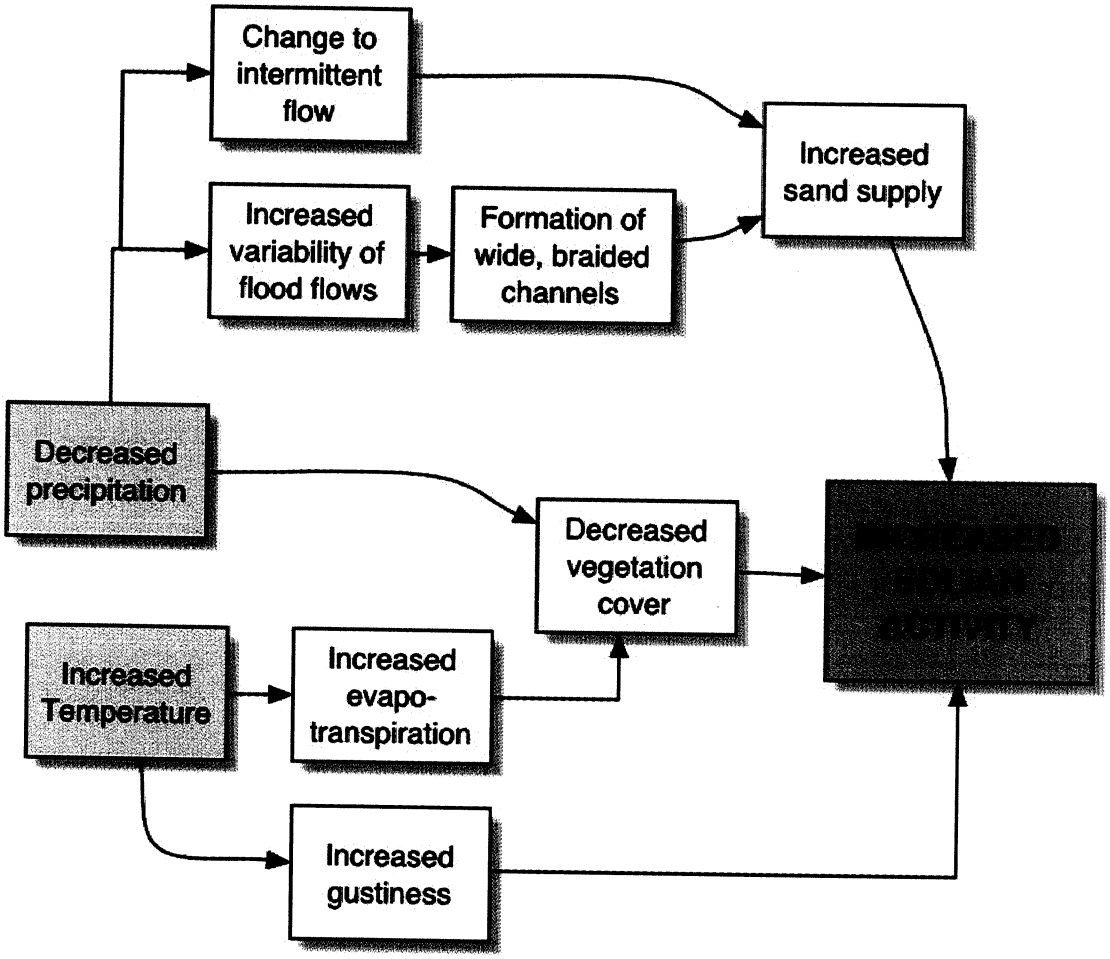

Figure 2.6: Process model of the effects of climate change on eolian activity in the High Plains, after Muhs and Holliday(1995)

Plains with a doubling in atmospheric CO_2 (Manabe & Wetherald, 1987; Gregory et al., 1997). Studies have suggested that greenhouse warming may result in a climate similar to that of the early to mid-Holocene (Hansen et al., 1988) when dune reactivation was more common. In addition to an overall likely decrease in moisture availability to the High Plains, an increase in the number of extreme events, such as droughts, has been predicted (Gregory et al., 1997; Overpeck et al., 1990).

2.3 Sand Transport Theory

A large amount of effort has also been spent in attempting to understand the controls on eolian geomorphology, beginning with Bagnold (1941). Much of this work has been spent learning about the physical processes that control sand transport. In general, the dominant controls on sand transport are wind speed, grain-size, and vegetation cover, though in some locations other factors such as soil moisture and cryptobiotic crust can dominate.

2.3.1 Bare Soil

The simplest case of sand transport is that which occurs on a flat, bare, sandy medium. In this case the primary controls are wind speed and grain-size. The seminal work of Bagnold (1941) laid the ground work for the physical understanding of sand transport by developing an empirical equation to predict the quantity of sand that would be transported in a given wind regime with a given grain-size. Further work has gone into understanding the physical processes of lift and drag that act on each grain of sand (fig.2.7), and more recently computer models have been created that can reasonably simulate the transport of a cloud of sand grains (Spies & McEwan, 2000).

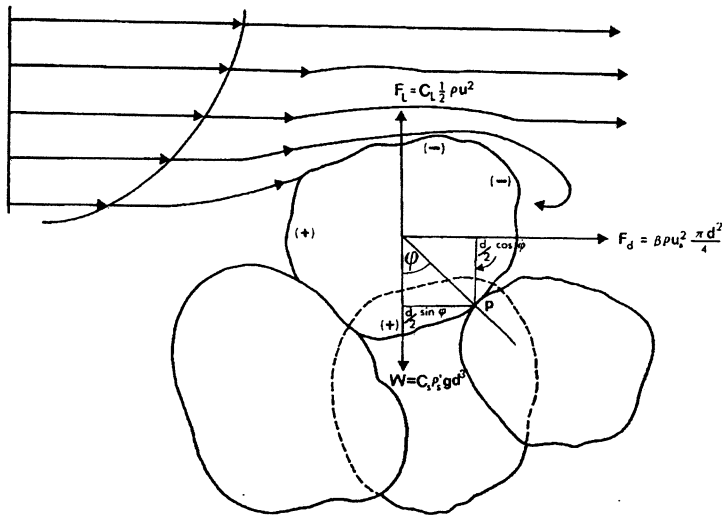

Figure 2.7: Physical processes controlling sand grain movement, after Pye and Tsoar (1990). A sand grain will be lifted off the bed if the difference in pressure above and below the grain exceeds the weight of the grain (W). F_L is the lift force, F_d is the drag force, C_L and C_s are shape coefficients, ρ is the density of air, ρ_s is the density of the grain, d is the grain diameter, and u is the wind speed.

Shear Stress vs Wind Speed

Wind speed is the most important factor in controlling sand transport on a bare, sandy surface. Under a laminar flow regime, wind speed varies logorithmically with height above a surface (fig.2.8), thus to understand the force that is acting on the surface itself it is necessary to calculate the shear stress (u^*) on the surface rather than the wind speed at some height above the surface. This is done by accounting for the roughness of the surface and the height at which a wind velocity measurement was made with Bagnold's (1941) wind profile equation (2.1). Where z is the measurement height, z_o is the surface roughness length, u_z is the wind speed at height z, and κ is von Karman's constant, 0.4. Ideally the roughness of the surface should be found by fitting Bagnold's equation through wind speed measurements at several heights; if this is not possible a roughness length must be estimated.

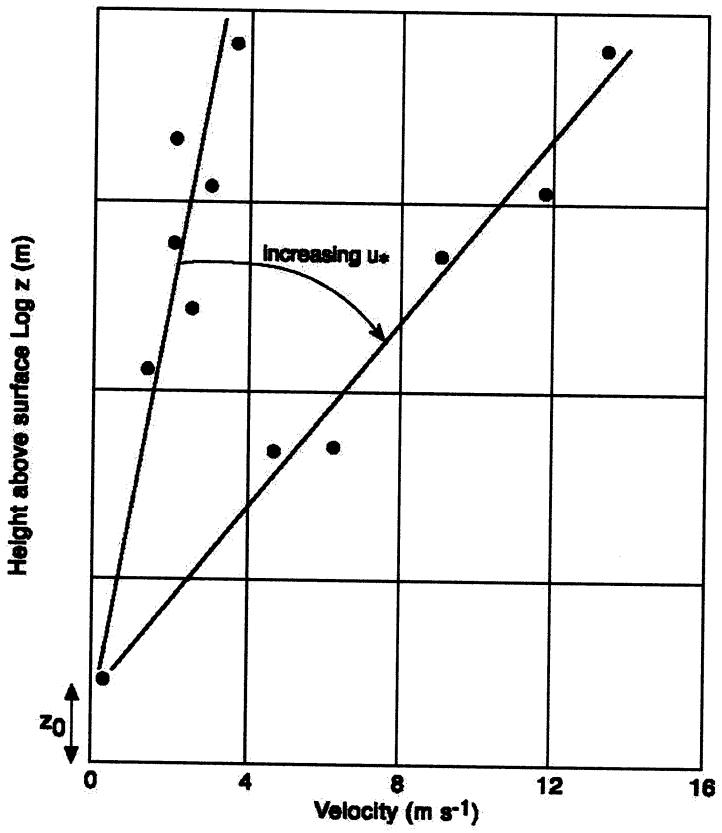

Figure 2.8: Typical wind profile with roughness length Z_0. Y-axis is the log of height above the surface, after (Wiggs, 1997)

$$u^* = \frac{\kappa * u_z}{\ln \frac{z}{z_o}} \tag{2.1}$$

Threshold Velocity

Below some wind speed there will not be enough energy to transport sand grains. This wind speed is known as the fluid threshold velocity (u_t^*). The threshold for a given grain size can be calculated by Bagnold's (1941) equation (eqn. 2.2). Where ρ_a is the density of air, ρ_s is the density of the solid particle, g is the acceleration due to gravity (9.8 $\frac{m}{s^2}$), d is the grain diameter, and A is an empirical parameter dependent on grain characteristics, roughly 0.1 for sand-sized

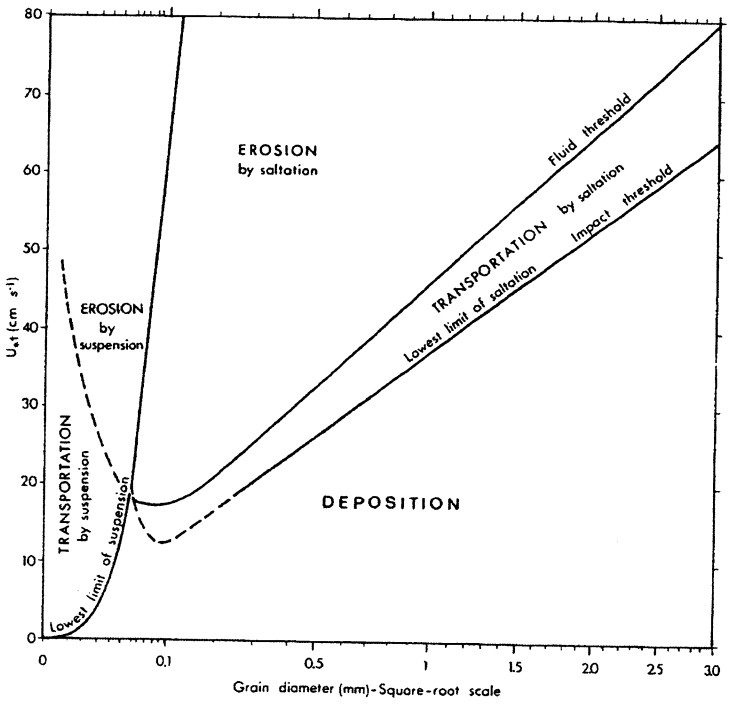

Figure 2.9: Fluid and impact saltation thresholds as a function of grain size, after Pye and Tsoar (1990)

particles. After the initiation of sand transport the effective threshold velocity decreases. When saltating sand grains land they impact the grains on the ground. At the instant of impact these grains are often lifted a little and thus the amount of wind required to maintain saltation is lower than the fluid threshold velocity. The velocity needed to maintain saltation is known as the impact threshold velocity and is lower than the fluid threshold (fig.2.9).

$$u_t^* = A\sqrt{\frac{\rho_s - \rho_a}{\rho_a} * g * d} \tag{2.2}$$

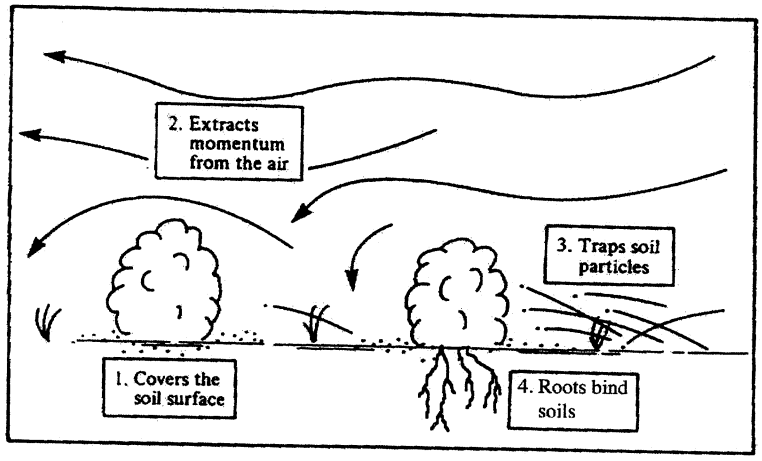

Figure 2.10: The effects of vegetation on sand transport, modified from Wolfe and Nickling (1993)

2.3.2 Vegetated Medium

Effects of Vegetation

Vegetation exerts four main effects on the potential for sand transport (fig. 2.10. Vegetation directly covers sand, thereby keeping the wind off of it. Vegetation makes the surface rougher, thus slowing down the wind near the ground. Vegetation roots provide a stronger medium than loose sand, and finally, vegetation blocks actively moving sand. Many researchers have attempted to quantify the effects of vegetation on sand transport. This work can be divided into main areas of research, theoretical models which work with generalized roughness elements (Gillette & Stockton, 1989; Musick et al., 1996; Raupach et al., 1993) and empirical models which have looked at vegetated mediums at specific field sites (Wasson & Nanninga, 1986; Stockton & Gillette, 1990; Hagen & Armbrust, 1994; Armbrust & Bilbro Jr., 1997; Lancaster & Baas, 1998). A good review of recent literature is given in Buckley (1998).

Theoretical Models

Many researchers have tried to focus on the more general problem of the effects of roughness elements on sand transport. By using simple shapes created from wooden blocks, rocks, or other readily mutable objects these researchers have hoped to further divide the problem into specific measureable components of roughness elements such as height, width, and porosity (Raupach et al., 1993). These techniques are advantageous because if a general solution could be created it could then be applied to any type of vegetation, fence, or other barrier. This work has had some success with simplified models, but has not scaled well to real vegetation due to the complexity of vegetation structure.

Empirical Models

The other main approach to predicting sand transport has measured movement in real world situations or in realistic labratory settings. Empirical approaches usually involve correlating wind speed and vegetation cover to sand transport in the field (Wasson & Nanninga, 1986; Stockton & Gillette, 1990; Hagen & Armbrust, 1994; Armbrust & Bilbro Jr., 1997; Lancaster & Baas, 1998) or in a laboratory setting (Buckley, 1987). This approach has the advantage that correlations are directly related to real world situations with real plants. It has the disadvantage that it is harder to control and results may only be significant for the exact sand, vegetation types at the given field site. Laboratory measurements such as Buckley (1987) are easier to control, but may not have realistic vegetation distributions, especially dead vegetation which can play an important role in covering sand. Field measurements such as Lancaster and Baas (1998) use real-world sites but as a result the researcher has little to no control over the vegetation cover or wind speeds. Field work usually yields weaker correlations

than laboratory research, but the inability to correlate variables from real field sites calls into question the utility of current laboratory measurements which are not reproducible in the field.

2.3.3 Large Scale vs Local Reactivation

All of these approaches to predicting sand transport focus on local conditions, but large scale reactivation may be controlled by other factors. Large scale reactivation requires that a downwind sink not immediately stop local sand transport, and local sites can be heavily influenced by upwind vegetation cover and sand transport. In addition a significant upwind source may be necessary for long term reactivation. Other studies have investigated larger-scale dune reactivation but have not developed equations which could reasonably be related to our study. Wiggs et al. (1995) correlated their dune activity index to measurements of vegetation cover (R^2=0.76) but did not include a measurement of wind speed in their study.

Climate Based Indices

In an attempt to take a larger scale approach several researchers have created climate based regional influences. The most commonly sited of these indices is the Dune Mobility Index of Lancaster (1987). The Dune Mobility Index (M) relates the percent of time wind speed is above the threshold for sand transport on a bare sandy surface (W_t) and the precipitation to potential evapotranspiration ratio (P/PE) to dune activity (eqn. 2.3, fig.2.11).

$$M = \frac{W_t}{\frac{P}{PE}} \tag{2.3}$$

Lancaster and Helm (2000) showed that the Dune Mobility Index for the previous year is correlated with the amount of sand transport at several field sites

in New Mexico and Arizona, but the slope of this relationship varies from 0.0007 to 0.5 (fig. 2.12). This variation in relationships shows that local factors can significantly alter the relative meaning of the index. While climatic indices give a broad picture of the likelyhood of dune activity they do not take account for localized variations in water resources and vegetation types, making them less useful for mapping regions of instability at the scale necessary for land management practices.

2.4 Measuring Vegetation from Landsat

Landsat data can be used to estimate the percent of vegetation cover at each point on the ground. This estimate is far from a perfect measurement. Landsat measures the amount of radiation received from within a specific angular instantaneous field of view. This includes radiation reflected and emitted by the atmosphere as well as radiation reflected and emitted by the ground surface. A modest correction was made in this study to account for variations in the atmospheric contribution over time, and emitted energy from the earth is, under most circumstances, several orders of magnitude less than reflected solar energy at wavelengths less than 2.5μm. Thus it is a reasonable assumption that most of the variation we see in Landsat data is due to variations in reflected solar energy, and in turn related to variability in ground cover.

The Normalized Difference Vegetation Index (NDVI) (Rouse et al., 1974) is a proxy for vegetation cover that can be derived from Landsat data. Vegetation typically reflects very strongly in the NIR and weakly in the red portion of the spectrum, while soil has a flatter reflectance curve, and senescent vegetation has an intermediate curvature (fig.2.13). Thus as the amount of vegetation within a given pixel increases the total NIR reflectance will increase, and NDVI with it. NDVI also removes the effects of variations in topography because it is a ratio

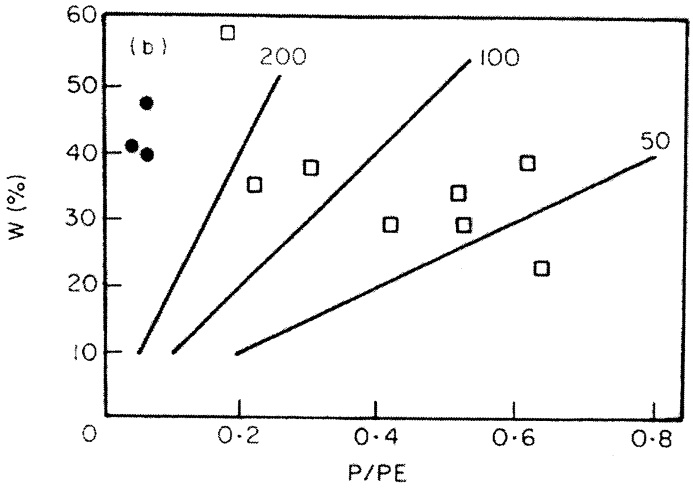

Figure 2.11: Dune Mobility Index graph of P/PE vs W_t. Locations with above a ratio of 200 are typically highly active, between 100-200 are slightly active, and below 100 are generally inactive. After Lancaster (1987)

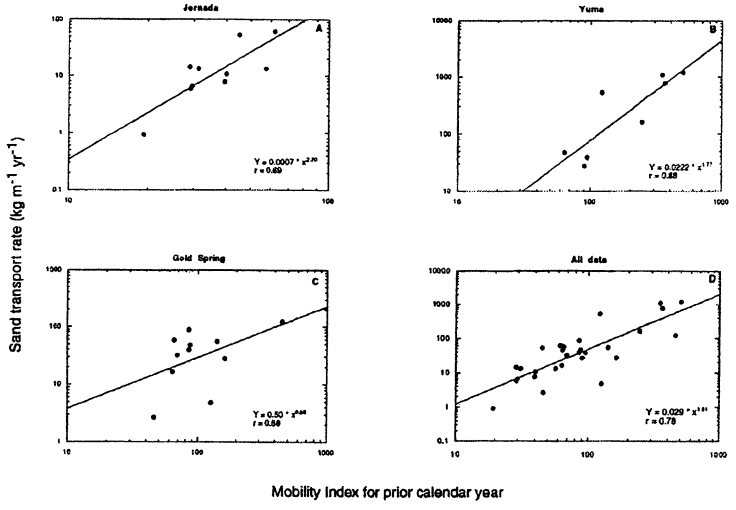

Figure 2.12: Correlation between Dune Mobility Index and measured sand transport at several sites in Arizona and New Mexico, after Lancaster and Helm (2000).

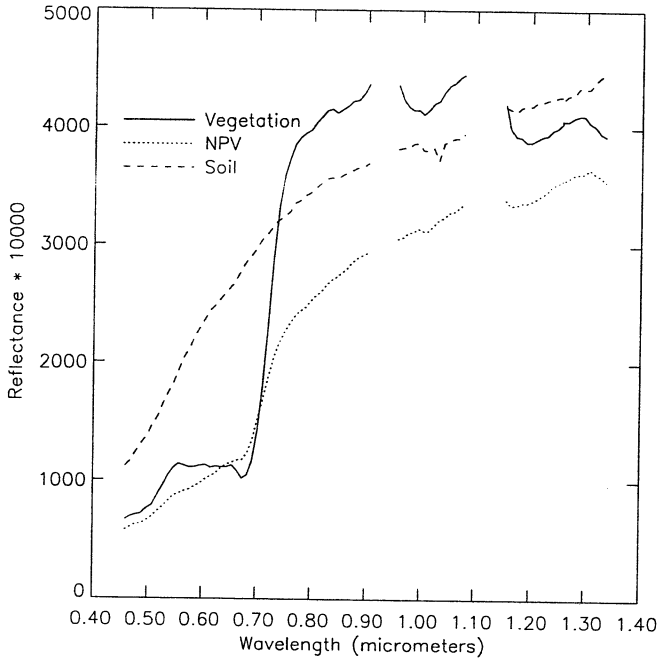

Figure 2.13: AVIRIS reflectance spectra for green vegetation, non-photosynthetic vegetation (NPV) and soil. The NDVI for these reflectance curves are approximately 0.59, 0.35, and 0.10 for green vegetation, NPV, and soil respectively. (Data from (Warner, 2000)

between two linear band combinations.

The variation in ground cover may not be limited to variation in the percent vegetation cover, thus at sensor radiance will be a function of variables other than vegetation cover. NDVI does not account for small variations in soil and vegetation reflectance. If soil types vary substantially the contribution of soil reflectance to NDVI can vary by as much as 0.3 (Huete et al., 1985). This means that NDVI measurements from different regions may not be directly comparable. NDVI is also sensitive to wet soil. Recent rainfall will significantly reduce the reflectance of soil and thus alter the NDVI over a wet region. The sensitivity to rainfall can make temporal analysis difficult. In addition, NDVI can be sensitive

to canopy geometry and non-photosynthetic vegetation (Wessman et al., 1997). Elmore et. al (2000) showed that spectral mixture analysis is a more accurate method of determining vegetation cover for temporal analysis than NDVI, but it is also requires very careful endmember determination in each scene.

2.5 Modelling Vegetation with CENTURY

The CENTURY ecosystem model version 4.0 was used in this study to relate vegetation cover to climate parameters. CENTURY was developed at Colorado State University to simulate nutrient cycling in temperate grasslands such as the High Plains (Parton et al., 1988). This model has been used heavily in ecosystem modeling studies (Gilmanov et al., 1997; Burke et al., 1997; Motavalli et al., 1994) including climate change scenarios (Parton et al., 1995). Version 4.0 of the CENTURY model runs on a monthly time step. The output parameters relevant to this study are aboveground live carbon, and standing dead carbon. More recently a daily time step version of the CENTURY model (DAYCENT) has been developed (Parton et al., 1998), but was not used in this study.

Chapter 3

Data and Methods

3.1 Landsat Images

This study incorporated over 100 Landsat images from thirty-three path/rows. These scenes were collected as part of the larger project at CSES to cover the Ogallala aquifer at three separate times. The data were selected in an attempt to include a variety of water stress levels. At least one image was collected in a drought year, and one in a normal to high precipitation year. Most path/rows have one scene from 1985, one from 1988 or 1989 and one from 1996. 1988 and 1989 were drought years in much of the High Plains. A few path/rows have been supplemented with a Landsat 7 scene collected in 1999. This temporal coverage allows analysis of the response of vegetation to water stress at each point in the High Plains for which we have cloud free coverage.

3.1.1 Information on Scenes

The thirty-three path/rows collected for this project cover the area from western Texas and southern New Mexico to southern South Dakota and Wyoming (fig. 2.1). Generally three to four separate dates for each scene were analyzed, although eight scenes were available for a detailed examination of eastern Colorado, scene 33/32 (tbl. 3.1).

Scene	Image Date
28/34	8/1/1988
28/34	7/22/1996
28/34	8/25/1985
28/36	8/1/1988
28/36	7/22/1996
28/36	8/25/1985
29/31	7/15/1985
29/31	7/26/1989
29/31	7/29/1996
29/33	7/15/1985
29/33	9/25/1988
29/33	7/29/1996
29/34	7/29/1996
29/34	7/31/1985
29/34	9/9/1988
29/35	8/14/1996
29/35	8/24/1988
29/35	7/31/1985
29/36	8/14/1996
29/36	8/24/1988
29/36	7/31/1985
29/37	8/14/1996
29/37	9/25/1988
29/37	7/31/1985
30/30	8/23/1985
30/30	9/3/1989
30/30	8/5/1996
30/31	8/15/1988
30/31	8/23/1985
30/31	7/4/1996
30/34	8/15/1988
30/34	8/5/1996
30/34	8/7/1985
30/34	9/7/1999
30/36	6/20/1985
30/36	8/21/1996
30/36	7/31/1994

Scene	Image Date
30/38	9/17/1994
30/38	6/20/1985
30/38	8/21/1996
31/30	10/1/1985
31/30	9/26/1989
31/30	8/28/1996
31/31	9/26/1989
31/31	7/27/1996
31/31	8/30/1985
31/32	9/26/1989
31/32	7/27/1996
31/32	8/30/1985
31/34	8/12/1996
31/34	7/28/1999
31/34	8/30/1985
31/34	9/7/1988
31/35	8/12/1996
31/35	7/19/1999
31/35	9/26/1989
31/35	8/30/1985
31/35	9/30/1999
31/36	8/12/1996
31/36	8/13/1999
31/36	9/26/1989
31/36	8/30/1985
31/37	8/12/1996
31/37	9/26/1989
31/37	8/30/1985
31/38	8/12/1996
31/38	9/26/1989
31/38	8/30/1985
32/30	8/19/1996
32/30	8/21/1985
32/30	7/31/1989
32/31	6/18/1985
32/31	7/22/1996
32/31	6/24/1993

Scene	Image Date
32/31	5/28/1989
32/32	8/21/1985
32/32	7/2/1996
32/32	9/7/1989
32/33	9/17/1989
32/33	8/21/1985
32/33	7/2/1996
32/34	9/17/1989
32/34	8/19/1996
32/34	9/30/1999
32/34	7/4/1985
32/38	9/17/1989
32/38	8/19/1996
32/38	7/4/1985
33/30	8/23/1989
33/30	8/26/1996
33/30	8/28/1985
33/31	8/10/1996
33/31	8/12/1985
33/31	9/24/1989
33/32	7/10/1999
33/32	8/12/1985
33/32	8/15/1992
33/32	6/15/1987
33/32	9/17/1998
33/32	9/24/1989
33/32	8/28/1985
33/32	10/5/1993
33/33	8/10/1996
33/33	9/24/1989
33/33	8/28/1985
34/30	8/17/1996
34/30	8/27/1988
34/30	7/2/1985
34/31	7/2/1985
34/31	9/15/1989
34/31	8/17/1996

Table 3.1: Landsat Images used in this study. Landsat scenes are refered to by their orbit path/row.

Geometric Correction

As part of the larger project at CSES, all scenes were registered to UTM zone 14. Originally all of the 1996 images were warped to vector layers such as roadmaps. The next step in the registration process required registering the remainder of the images to the 1996 images. To do this, one rough warp, based on hand picked ground control points, was performed, followed by a more rigorous registration performed with the IMCORR program (Scambos et al., 1992) which typically generates sub-pixel accuracy. Registration was performed with a nearest neighbor resampling.

Radiometric Calibration

Radiometric calibration is essential for accurate analysis of multi-temporal data as well as for meaningful comparisons between scenes. Satellites such as Landsat measure radiance at the sensor. Within each spectral band (λ), at sensor radiance (L_λ) varies dominantly as a function of surface reflectance (ρ_λ), solar irradiance ($E_{o\lambda}$), atmospheric transmission down ($\tau_{\lambda\downarrow}$) and up ($\tau_{\lambda\uparrow}$), the angle between the ground surface normal and the incoming solar irradiance (θ), and path radiance ($L_{p\lambda}$) (eqn. 3.1), the subscript λ indicates a wavelength dependent parameter. Landsat data for the 1996 imagery were converted to radiance using the published Landsat gain and offset. These data were then converted to apparent reflectance by computing solar irradiance from the sun angle and distance at the time of acquisition (from Landsat 7 Data Users Handbook), and estimating path radiance based on the dark object subtraction method (Chavez, 1996). This method does not remove the effect of variations in topography represented by $\cos(\theta)$, these variations are accounted for in the NDVI calculation.

$$L_\lambda = \frac{\rho * E_{o\lambda} * \tau_{\lambda\uparrow} * \tau_{\lambda\downarrow} \cos(\theta)}{\pi} + L_{p\lambda} \tag{3.1}$$

The remainder of the imagery was then cross calibrated to the 1996 reflectance imagery. An advanced pseudo invariant features technique was used to calibrate each scene. A spectral angle map (SAM) was created by calculating the dot product between the spectral vectors of each pixel from two scenes. From this map the pixels with the smallest change in spectral angle were taken to be pseudo invariant (their surface reflectance was assumed to be unchanged). For each spectral band, the pixels from the image to be calibrated were regressed against the corresponding pixels from the 1996 imagery to calculate an image to image linear calibration. While this calibration process does not entirely remove atmospheric effects it does attempt to remove differences in atmospheric effects between dates. This method does not account for atmospheric variability between different path rows, only between dates for a single path row.

3.1.2 NDVI

The Normalized Difference Vegetation Index (NDVI) is a useful measurement of vegetation that can be derived from Landsat TM and ETM+ data. NDVI is calculated as the difference between Near Infrared (NIR) and red reflectance divided by the sum of NIR and red reflectance (eqn.3.2). This method removes topographic variability because the $\cos(\theta)$ term from equation 3.1 cancels out when you compute a ratio of radiances, this assumes the path radiance has been properly removed first.

$$NDVI = \frac{NIR - Red}{NIR + Red} \tag{3.2}$$

3.1.3 Spatial Resolution

To analyze the importance of spatial resolution, Landsat imagery from eastern Colorado and the Nebraska sand hills were resampled to common lower resolutions. MODIS and AVHRR are two sensors which could potentially be used

in place of Landsat at less cost and with a higher temporal resolution. Landsat pixels are 30m across, AVHRR pixels are 1000m, and MODIS has 250m pixels. This means that there are over 1000 Landsat pixels for each AVHRR pixel, and just under 70 Landsat pixels for every MODIS pixel. Landsat data were averaged together to produce simulated AVHRR and MODIS pixels eastern Colorado and Nebraska.

3.2 Ancillary Data

3.2.1 Soils Map

A sandy soils map was created based on the 1:250,000 National Resource Conservation Society (NRCS) State Soil Geographic database (STATSGO) using the map of eolian sand in the High Plains presented by Muhs and Holliday (1995) as a template(fig. 2.1, 3.1). The STATSGO map is divided into a number of classes, none of which is clearly eolian sand. Soil types from the STATSGO map which appeared to fall within an area designated by Muhs and Holliday (1995) as eolian sand were treated as such. The final classes used from the STATSGO database are "Sandy", "Siliceous", "Arenic", "Aridic Paleustalfs", "Ustic Torripsamments", and "Ustipsamments" (Mesic and Mixed). Some further hand editing was then applied to match individual regions that were on the Muhs and Holliday map. This step was necessary to generate a detailed, geographically rectified map for model input.

3.2.2 Rangeland Map

As part of a larger project at CSES a map of cloud free rangeland across the High Plains was hand digitized. This map was created by outlining cloud free rangeland in one year for a given path/row then editing that file to exclude any

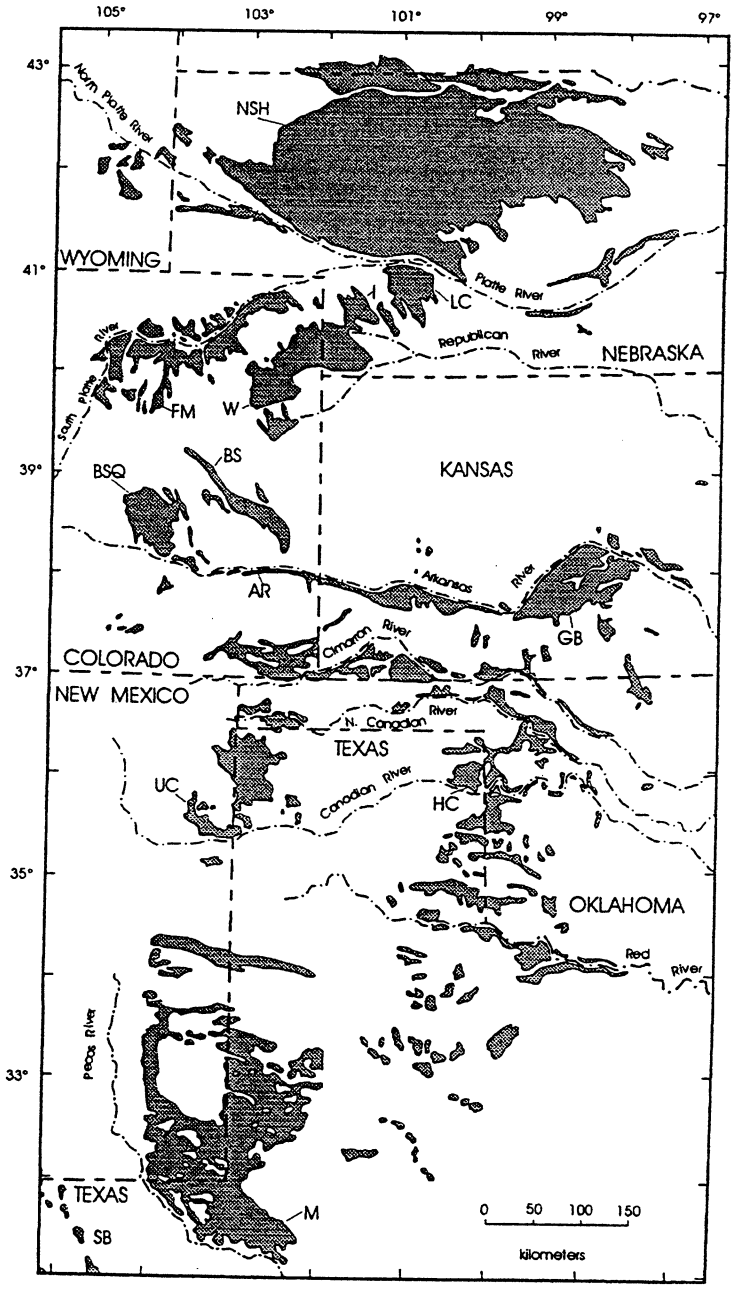

Figure 3.1: Muhs and Holliday (1995) map of eolian sand. This map was used as a template to generate a map of sandy soils from the STATSGO database (fig. 2.1)

areas that were covered by clouds on other dates. Rangeland was grossly defined to cover any area that was not farmed or substantially built-up. This includes areas which are grazed as well as other, more natural areas. For simplicity, this map includes bed rock, dry lakes, and other features which are clearly non-eolian. Ideally the sandy soils map or the rangeland map should eliminate these regions because their presence will interfere with the statistics of the correlation between NDVI and CENTURY values. Since these odd areas are separated during the classification process and cover a relatively small area, they should not substantially alter the final results.

3.2.3 Climate Data

Precipitation and temperature data were acquired from a large National Climate Data Center (NCDC) database (EarthInfo, 2000). This database includes the climatic data required to run the CENTURY vegetation model. Only weather data that was continuous from 1971 to the final date required for the imagery was used. Most data began around 1950 and some records began before 1900. The data base is made up of daily measurements, but, because CENTURY is only run on a monthly time step, the data were averaged into monthly values.

3.2.4 Wind Data

Wind data were taken from the U.S. Air Force Combat Climatology Center's (AFCCC) DATSAV2 Surface Hourly database. These data are gathered at a standard 10m height above the ground. Wind measurements are recorded hourly in this database. The maximum wind speed in each month was calculated for each station. The mean of these maximums was then calculated to generate a simple statistic that represents the average maximum wind speed, referred to here as the Mean Monthly Maximum.

Conversion to Shear Velocity

To make these measurements useful to the calculation of sand transport they were converted to shear velocity. Shear velocity is a measure of the influence wind has on the ground surface, and most studies of sand transport relate sand transport to wind shear velocity (u^*). The roughness around each station was unknown, but was assumed to be relatively smooth, a roughness length of 0.0005m (z_o) was assumed. Roughness length has less effect on wind measurements made around 10m, because the term $\ln(\frac{z}{z_o})$ is insensitive to small perturbations in z_o at large values of $\frac{z}{z_o}$. Most of the effect appears in the lower boundary layer, thus a smooth roughness length is a reasonable assumption for these data. Shear velocity was then calculated by equation (eqn. 3.3).

$$u^* = \frac{\kappa * u_z}{\ln \frac{z}{z_o}} \tag{3.3}$$

Where z is the measurement height (10m), u_z is the wind speed at height z, and κ is von Karman's constant, 0.4.

Spatial Interpolation

To generate a wind map, these measurements were krigged for each path/row. All available wind measurements were searched to find any that existed within 100km of the path/row boundaries. This typically yielded nearly 10 stations. The Mean Monthly Maximum was computed for each and krigged (Isaaks & Srivastava, 1989). Kriging was performed with IDL's Krig2D function using the spherical option to fit the semi-variogram, and a large range. The range was set at one half the size of the Landsat image. To speed numerical computation, kriging was performed at a 300m grid size rather than a 30m grid size.

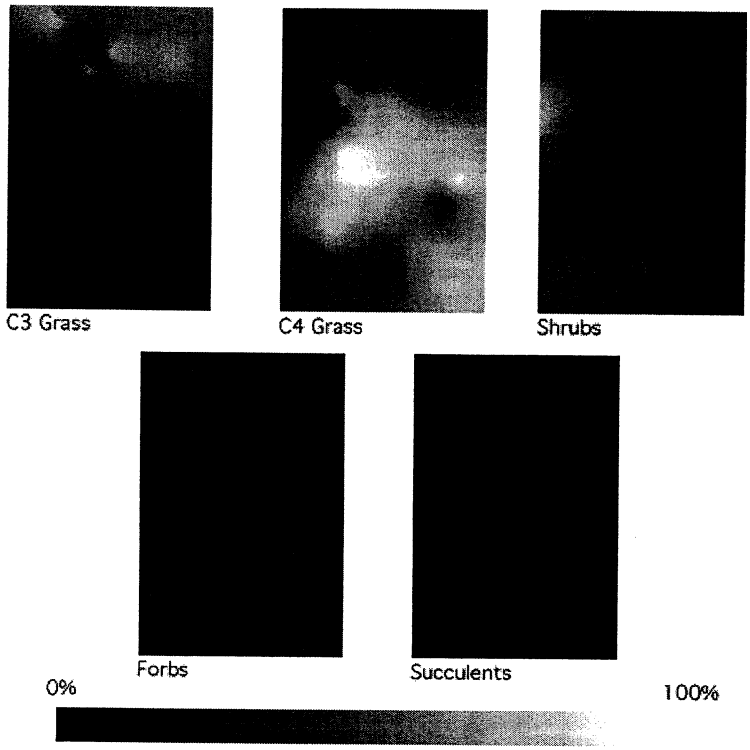

Figure 3.2: Vegetation type maps generated by kriging data points from Paruelo and Lauenroth (1996).

3.2.5 C3 vs C4 Grassland Map

A map of grass types across the High Plains was generated using published values of vegetation types from 73 locations across the Plains (fig. 3.2). Paruelo and Lauenroth (1996) compiled a list of vegetation types at 73 locations from published papers. They split vegetation types between C3 grass, C4 grass, shrubs, forbs, and succulents. All of these categories were krigged across the High Plains to generate an approximate map for the entire area. To simplify this further I classified succulents and shrubs as C4 and forbs as C3. Though shrubs are often C3 and succulents actually use a third photosynthetic pathway (CAM) they were lumped in with C4 grasses because they, like C4 grasses, respond more slowly to water stress. All five of these categories were normalized to sum to one and the

Century Crop Parameter	% C3 Grass associated with Crop
CPR	100
G4	75
G3	50
G5	25

Table 3.2: Main CENTURY grassland types

percent of C3 plants was calculated for each grid point (eqn. 3.4).

$$\%C3 = \frac{C3 + forbs}{C3 + forbs + C4 + shrubs + succulents} \tag{3.4}$$

3.3 CENTURY Modeling

The CENTURY model (Parton et al., 1988; Metherell, 1992) was used to model vegetation abundance across the High Plains. The CENTURY model incorporates vegetation type, soil type, and real weather to model vegetation growth. For this study, I used CENTURY Version 4. CENTURY model runs were performed at all points across the High Plains for which suitable weather data were available.

3.3.1 Parameterization

C3 vs C4

The percent C3 and C4 grass was specified in all CENTURY model runs by using one of the base parameterizations provided. Built into the CENTURY model are 4 classifications of varying C3 vs C4 abundances (tbl. 3.2). For each station that was to be simulated in CENTURY the percent C3 was determined from the C3 vs C4 grassland map mentioned above and the appropriate parameterization was used for that CENTURY run.

Weather

The climate data from the NCDC database were used to parameterize CENTURY. Daily weather data were converted to monthly averages for all available years. In addition, complete monthly means, standard deviations, and skewnesses were calculated to allow CENTURY to generate weather stochastically. This stochastic weather is used to spin up the model for 2000 years. This allows the model to reach an equilibrium with the local climate before trying to match the actual weather data.

Soils

CENTURY modeling was only performed for sandy regions. All CENTURY model runs were parameterized to run with eighty percent sand, ten percent clay, and ten percent silt. In reality this parameter varies spatially, but because sufficient soil maps were not available. Because the only areas I was interested in in the end are sandy regions, this assumption is considered reasonable.

3.3.2 Interpolation

CENTURY version 4.0 is a point specific model, thus to generate a map of modeled vegetation it was necessary to interpolate between point locations. CENTURY could only be run at locations for which a viable weather record was available, thus there were a limited number of points available. These points were interpolated spatially with IDL's Krig2d function using spherical kriging, and a range equal to half of the height of the image. Each path row was krigged separately using any CENTURY points located within ten kilometers of the image boundary.

3.4 CENTURY vs NDVI

NDVI values were regressed against CENTURY output values in an attempt to correlate vegetation cover to weather at each point on the ground. To get a better estimate of NDVI, large areas of similar vegetation cover were averaged together, these areas were determined by a classification process described below. NDVI is influenced by the amount of non-photosynthetic vegetation as well as green vegetation. To account for the influence of non-photosynthetic vegetation half of the CENTURY output variable stded (standing dead carbon) was added to the CENTURY value for aglivc (above ground live carbon). This final value was regressed against NDVI.

3.4.1 Temporal Classification

To find areas of similar vegetation, NDVI time sequences were classified with the ISO-data classifier. Details of the ISO-data classifier can be found in Tou and Gonzalez (1974). All available NDVI images for a given path row were concatenated together and masked to eliminate areas that contain clouds, non-sandy soils, or have been heavily influence by humans. The resulting image was classified on the basis of the time variance of NDVI at each pixel. Each class in the resulting image should represent a group of pixels in which the vegetation responds similarly to recent weather. To investigate the importance of the number of classes used, the classifier was initialized with 5, 10, 15, 20, 25, 30, 35, and 40 classes in separate runs. Each class was required to have at least 1000 pixels in it. The classifier was allowed to join and seperate classes to find the optimal clusters, and the classifier was run for three iterations.

3.4.2 Correlation

From the maps generated by interpolating CENTURY values for agliv and stded, it was possible to correlate NDVI with CENTURY both spatially and temporally. This regression model tries to find the correlation for each class of ground cover mapped by the ISO-data classifier. Every reference to correlation is on a class by class basis. To look for the combination of spatial and temporal relationships, NDVI values were regressed against every corresponding CENTURY value within a class. This form of correlation has a data point for every pixel in every available image. To look for temporal correlation, all of the NDVI values in each ISO-data class were averaged together, as were all of the CENTURY values; this generates a single point for each date of available imagery. Each of these averages was computed for each date of Landsat imagery available and the results were regressed with ordinary least squares regression. Because most scenes only have three years of imagery the temporal regression is severely limited in the number of data points, therefore, the combined spatial and temporal correlation was used for the model output. The temporal correlation was used to investigate the impact of the number of classes and the number of images used in the regression.

3.5 Future Vegetation

A future vegetation map was generated based on the correllation between NDVI and CENTURY for each class. A potential extreme drought CENTURY value (30g Carbon) was used with the regression developed previously to estimate NDVI for each class during an extreme drought. This value was then converted to vegetation cover by assuming that the minimum and maximum two percent of NDVI values from the original Landsat imagery correspond to 0% and 100% vegetation cover respectively and interpolating between those values. Because

the correlation in some of the classes was negative or had an extremely low R^2 value a statistical method was used as a fall back estimate of vegetation cover. If the correlation was deemed spurious, the average NDVI value for a class was calculated and divided in half to represent drought conditions.

3.6 Sand Transport

A potential sand transport map was generated based on the future vegetation map and the wind map. At each pixel the equation derived by Lancaster and Baas(1998) (eqn. 3.5) was used to estimate potential sand transport.

$$q = 300 * (u_* - u_{*t})^3 * e^{-25*\lambda} \tag{3.5}$$

where :

q = Total sand flux ($gm^{-1}s^{-1}$)

u_* = Wind shear velocity

u_{*t} = Threshold shear velocity

λ = Vegetation cover

3.7 Model Overview

The entire sand transport model is illustrated in figure 3.3. Precipitation and temperature data are used in conjunction with maps of vegetation type and soil type as inputs to the CENTURY vegetation model to predict potential vegetation across the High Plains. Separately, Landsat measurements of vegetation (NDVI) are classified to map areas of similar ground type. A time series of NDVI measurements for each of these ground types is correlated with a time series of potential vegetation predicted by CENTURY. These correlations are used to predict vegetation cover for each class of ground type in a drought scenario. This

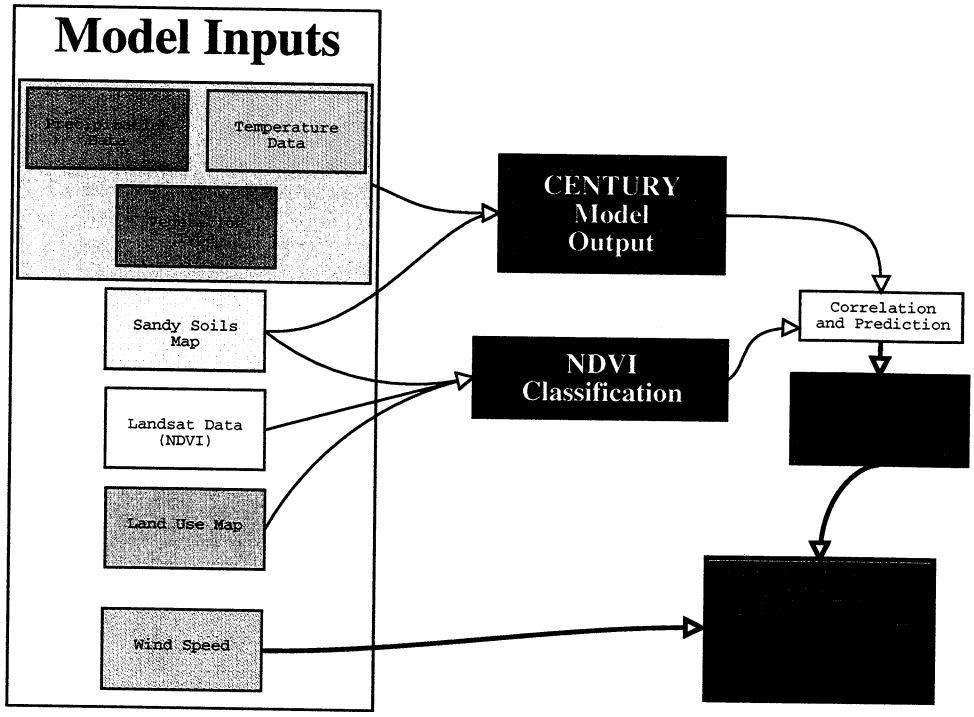

Figure 3.3: Sand transport model overview. Basic model inputs are on the left, the process is described in detail in the text.

map of future vegetation is then combined with a map of present wind speeds to predict potential sand transport across the High Plains.

Chapter 4

Results

4.1 Areas of Apparent Instability

According to this model, the largest areas of potential instability are the Nebraska Sand Hills, and portions of eastern Colorado, New Mexico and Texas (fig. 4.1). Isolated locations through out the High Plains also appear to be at risk, but no place else has as large an area which appears likely to reactivate.

4.1.1 Areas with Clear Dune Landforms

Many of the areas that this model mapped as having a high potential for reactivation exhibit clear eolian land forms. One would expect that locations that have experienced recent sand activity would be the most likely to reactivate in the near future. The region south of the South Platte river in Eastern Colorado has many clear parabolic dune forms (fig 4.2), evidence that this region has been active many times in the past. Areas here that are mapped with an extremely high reactivation potential are commonly semi-active today with numerous blowout features. For the areas in Eastern Colorado multiple model runs were analyzed, in all cases these areas were mapped with a high reactivation potential.

Other areas that were mapped with a high potential for reactivation include the Nebraska Sand Hills, and portions of western Texas and eastern New Mexico. The Nebraska Sand Hills are large transverse dunes (fig. 2.4), and many of the

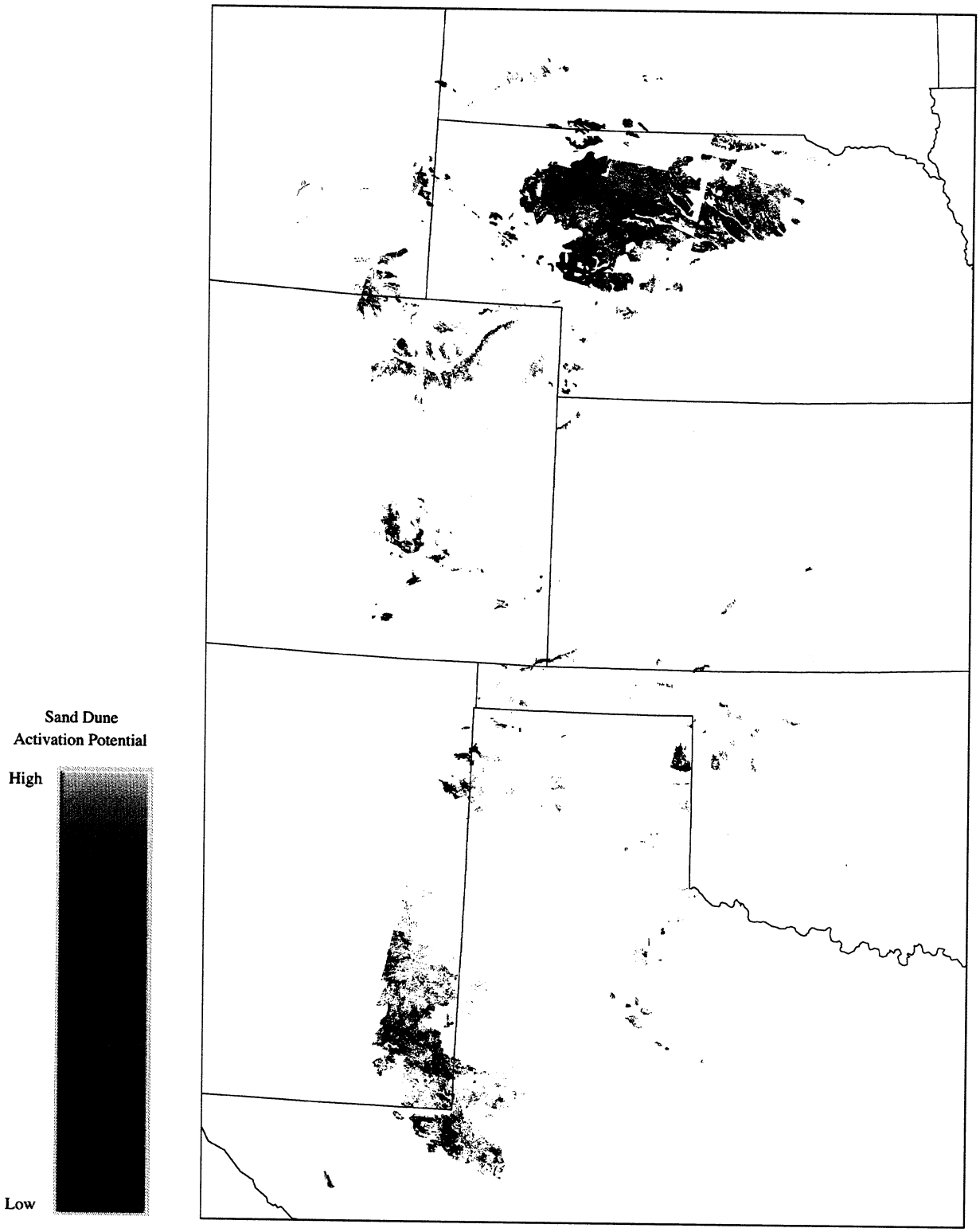

Figure 4.1: Potential sand dune activity map for the entire High Plains. Color scale indicates potential for sand dune activity. White designates areas with negligible activation potential and regions that were not mapped by this study.

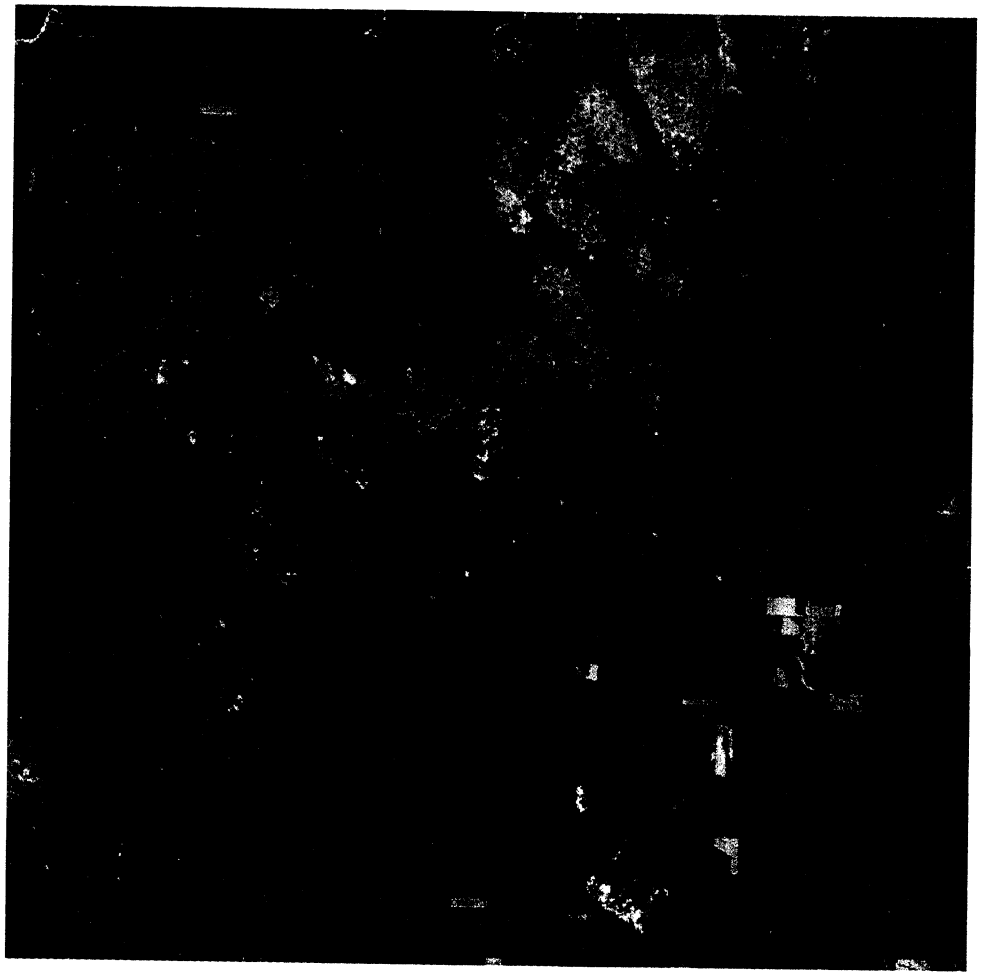

Figure 4.2: Parabolic dunes are common in Eastern Colorado. This area, South East of the South Platte river, shows a various levels of dune activity. The parabolic shapes in this images are only moderately elongated.

locations in Texas are currently active sand dunes (fig. 2.2).

4.1.2 Areas with Clear Non-Eolian Landforms

Some areas that were mapped as having a high potential for reactivation actually exhibit non-eolian land forms. One area in particular in Eastern Colorado shows clear fluvial erosional features (fig. 4.3). This area fell with in scene 33/32, thus eight images were available for the model. The sensitivity analysis used to study the effect that the number of available Landsat images had on the model

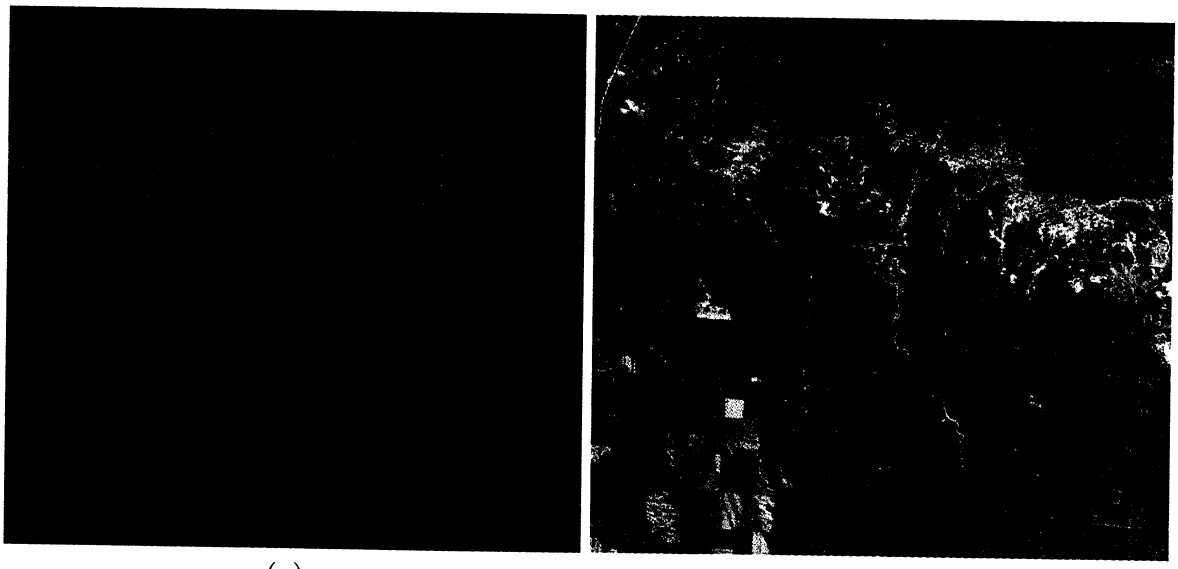

(a) (b)

Figure 4.3: This section of Northern Colorado has sections mapped with a high reactivation potential (red and yellow, [a]). Examination of a CIR Image of the areas shows clear fluvial features [b].

showed mixed results for this area, but the bright stream bed was always mapped with a high potential for reactivation.

4.2 NDVI vs CENTURY Correlation

In general the correlations between NDVI and CENTURY modeled vegetation cover were poor. The coefficient of determination was calculated for each class in each scene, for all points, and for temporal correlation. The number of classes used by the model was allowed to vary from 5-50, and the coefficient of determination was calculated to analyze the effects of this modification in the number of classes. For scene 33/32 the coefficient of determination was also calculated with varying numbers and dates of input scenes.

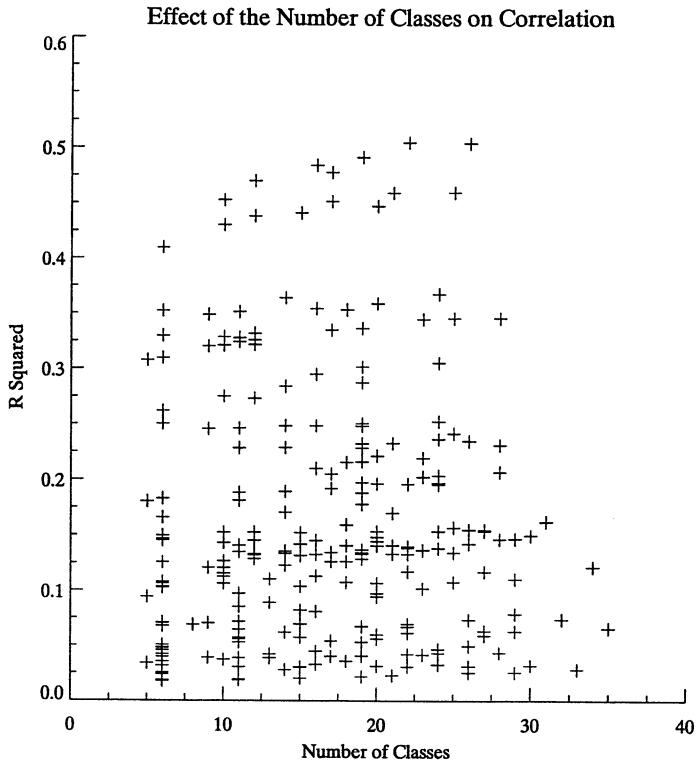

Figure 4.4: Coefficient of determination from temporal regression of NDVI to CENTURY plotted against the number of classes used to seperate different ground types.

4.2.1 Sensitivity to the Number of Classes

There was no apparent trend in the degree of correlation between NDVI values and CENTURY values due to the number of classes in the model. The coefficient of determination was graphed against the number of classes for all points, and for the temporal correlation alone (fig. 4.4).

4.2.2 Sensitivity to Temporal Resolution

In scene 33/32 it was possible to analyze the effect that the number of available Landsat images has on the degree of correlation between NDVI and CENTURY. Random images were chosen for 3-7 image subsets. There was an

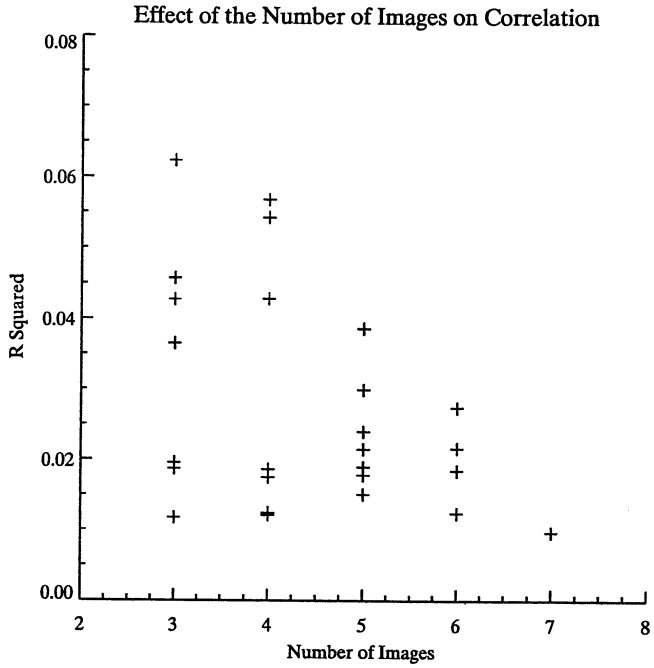

Figure 4.5: Coefficient of determination from regression of NDVI vs CENTURY, plotted against the number of images used in the model.

apparent decreasing relationship between the amount of variation explained by CENTURY with an increasing number of input images (fig. 4.5). This is probably due to the fact that with only three images it is very easy to get a spurious correlation. Examination of the p-values from the F-test shows no correlation between quality of fit and the number of images (fig. 4.6).

4.3 Spatial Resolution

Landsat images which were spatially averaged to simulate AVHRR and MODIS imagery show a substantial loss in detail. In eastern Colorado dune crests are blurred in MODIS imagery, but crop circles are still resolved(fig. 4.7b). AVHRR pixels sizes do not definitively distinguish between sparse agriculture and open rangeland, and dunes are completely obscured (fig. 4.7c). In Nebraska

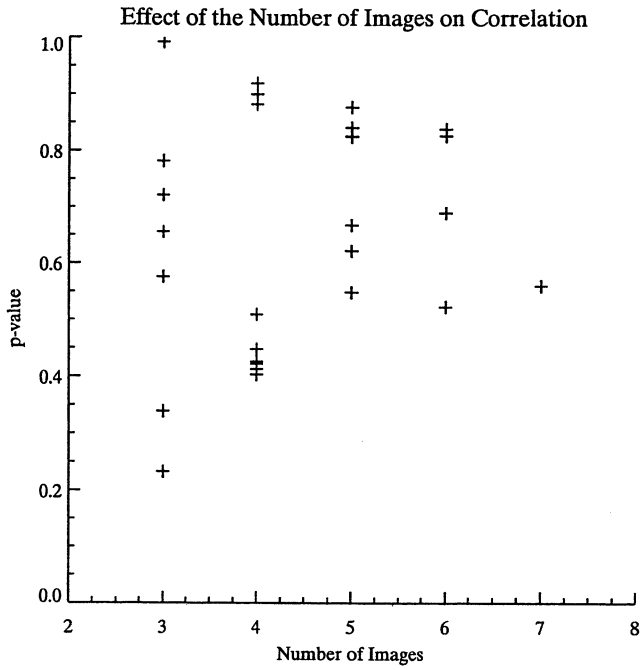

Figure 4.6: The average F-statistic p-value for the temporal correlation of NDVI and CENTURY, plotted against the number of images used in the model.

MODIS data are able to clearly distinguish major transverse dune features and separate the large, heavily vegetated interdune areas from the dune crests (fig. 4.8b). In this same area AVHRR is unable to resolve the dune crests, thus large, potentially unstable dunes are averaged together with heavily vegetated interdune areas (fig. 4.8c). Note that although it is possible to resolve the major transverse dunes in Nebraska with MODIS, it is not always possible to differentiate lakes from dune crests. However, this would be easy to do in a CIR image. It is important to note that these represent best case scenarios for both MODIS and AVHRR with perfect sampling, and extremely low noise because they are the result of averaging Landsat pixels together, real AVHRR and MODIS data would have much more noise, and delineation of features that are only one pixel wide would become harder.

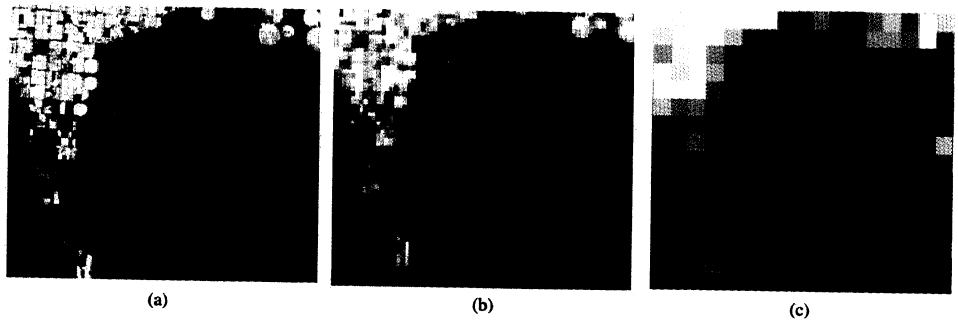

Figure 4.7: Low spatial resolution imagery in eastern Colorado shows the limitations of the MODIS and AVHRR sensors. a) is the original Landsat image, b) is the Landsat image resampled to MODIS (250m) pixel size, and c) is the Landsat image resampled to AVHRR (1km) pixel size.

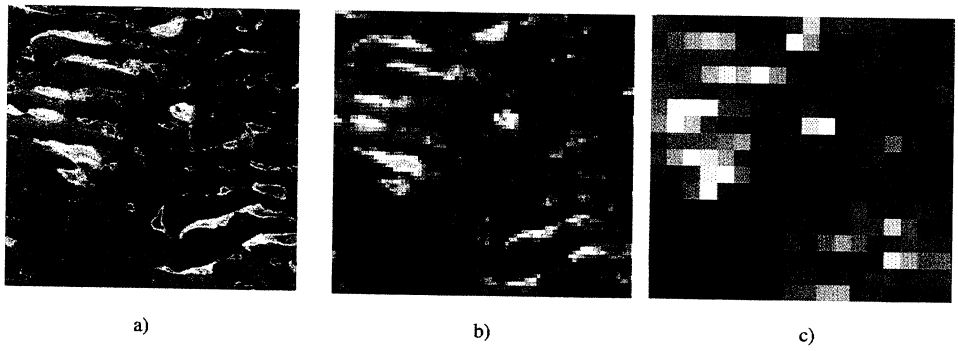

Figure 4.8: Low spatial resolution imagery in the Nebraska sand hills shows the limitations of the MODIS and AVHRR sensors. a) is the original Landsat image, b) is the Landsat image resampled to MODIS (250m) pixel size, and c) is the Landsat image resampled to AVHRR (1km) pixel size.

Chapter 5

Discussion

5.1 Vegetation Measurement

Neither NDVI nor CENTURY represent a perfect measurement of vegetation. NDVI values within rangeland were assumed to be unaffected by any processes other than vegetation growth due to weather and localized conditions such as topography, which are assumed to be time invariant. This is clearly not the case as much of the area is grazed in a time variant fashion, and recent rain can strongly effect NDVI values by darkening the soil. CENTURY values are modeled vegetation estimates which are completely dependent on the parameterization of the model.

5.1.1 Grazing

Areas that are heavily grazed pose a problem to this study. From Landsat data, it is impossible to readily distinguish areas which have been grazed from areas which have not. Heavy grazing during a wet year and a lack of grazing during a dry year may cause the vegetation at a given locality to apparently respond inversely to what would be expected under climatic forcing alone. The effects of grazing are clearly present in the images. Occasionally fence lines are visible due to differential grazing patterns (fig. 2.5). A tighter integration of land use studies could possibly alleviate some of these problems as it is possible to

include grazing in the CENTURY model.

5.1.2 NDVI

NDVI is not necessarily directly correlated with vegetation cover. NDVI is based on the variation in apparent reflectance between the red portion of the spectrum and the NIR portion (fig. 2.13). Because vegetation has a much higher difference in reflectance between the NIR and red than soil, a simple measure of this difference is often highly correlated with the amount of vegetation cover in a pixel; this is especially true for arid environments. Numerous studies have shown that Leaf Area Index (LAI) varies linearly with NDVI for LAI values less then 2-3, depending on leaf angle, and then approaches some maximum value asymptotically (Tucker, 1979; Asrar et al., 1984; Nemani & Running, 1989; Carlson et al., 1990; Carlson & Ripley, 1997). And LAI and fractional vegetation cover are also strongly related, as illustrated by Carlson and Ripley (1997) . However, different soil types can have different NDVI values, and within a specific soil type NDVI can vary substantially due to moisture content. Because this model is only designed for sandy soils the variability of NDVI due to varying soil type is probably not very large, but it could still be significant. The variability in NDVI due to soil moisture is much harder to account for and may be a large source of error in this study. Soil moisture decreases NIR reflectance, thus lowering NDVI for a region. Summer thunderstorms are common in the High Plains, and can be highly localized and ephemeral, making it difficult to account for, especially at the scale of Landsat. Given a map of rainfall prior to each Landsat scene a mask could be generated to throw out any NDVI values which are likely to have been effected.

5.1.3 CENTURY

CENTURY model output may not be representative of vegetation cover at the time of a Landsat overflight. The CENTURY model has been show to be accurate within 25% in areas of semi-arid grasslands (Parton et al., 1993), but it may be prone to substantial errors due to imprecise parameter estimates. Because this study has attempted to extend CENTURY measurements over a broad area certain weaknesses are inherent to our use of it. It was not possible to verify every measurement location to determine exact soil type, nutrient conditions, or vegetation types, thus our estimations of these quantities stem from a general sandy soil estimate, and a vegetation map generated from point values spread across the High Plains. In addition, CENTURY output is on a monthly basis. Landsat measures vegetation at a single point in time. Recent rainfall may have allowed substantial vegetation growth in the days leading up to a Landsat overflight. Herbaceous vegetation can respond very rapidly to rainfall events and change on this time scale is not predicted with CENTURY's monthly time step.

Vegetation type

Vegetation type is a very important parameter in CENTURY which may be improperly estimated in this study. Vegetation type determines how efficiently plants use water and nutrients. C4 plants tend to be much better at conserving water than C3 plants due to their specialized photosynthesis process. To attempt to include this variability in the CENTURY model, a map of C3 vs C4 vegetation type was created from points compiled by Paruelo and Lauenroth(1996) (fig. 3.2). The points compiled in this paper actually refer to C3 grasses, C4 grasses, forbs, shrubs, and succulents. CENTURY does not explicitly model forbs or succulents, though it can model shrubs. Because of the added complexity involved in modeling

shrubs, this model further simplifies everything into C3 or C4 grasses. Forbs typically use the C3 photosynthesis pathway, thus they were lumped into C3. Shrubs commonly use the C3 pathway, but respond more slowly to changes in precipitation so they were lumped as C4. Succulents use a third photosynthetic mechanism classified as CAM. Because the CAM pathway is more similar to the C4 pathway, succulents were also lumped into the C4 group. This lumping is partially justified by the fact that the based on the maps in figure 3.2, forbs and succulents appear to play a relatively minor role, and even shrubs are only dominant in a few locations.

This classification into C3 and C4 vegetation type throws out some of the information available; a better model may result from more detailed vegetation classification. Forbs typically respond more rapidly to rainfall, and have a strong influence on NDVI, so their inclusion as C3 may underestimate changes in NDVI over time, especially if there has been very recent rainfall. Succulents and shrubs, on the other hand, typically respond much more slowly to variations in climate than do C4 grasses, thus lumping them in with the C4 class may increase CENTURY's response time for vegetation due to weather forcings. In addition, the spatial estimate of vegetation type is based on the assumption that vegetation type varies smoothly across the High Plains. This is certainly not the case as vegetation type often varies substantially due to localized variability in water and nutrient availability, not to mention human influence.

Soil Type

CENTURY also provides for detailed soil parameterization. Because we were limiting this model to areas of sandy soil, all CENTURY runs were performed with 80% sand, 10% clay, and 10% silt. The STATSGO Database used to derive areas of sandy soil includes more detailed information on soil types, but there is

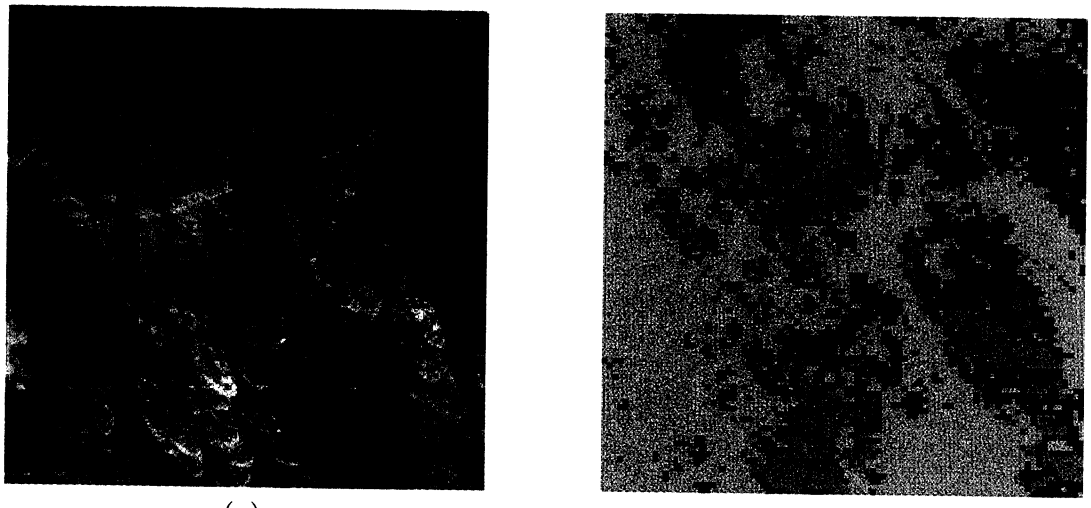

(a) (b)

Figure 5.1: Comparison of a high spatial resolution image (a) (Ikonos 4m CIR composite) to a classification developed from a time series of Landsat (30m) NDVI measurements (b). The yellow class indicates relatively stable ground, the red class represents areas that are partially stabilized, and the gold class represents areas that are nearly active today.

no clear mapping between their soil types and CENTURY's soil types. This is an area that could potentially be improved in the future with a careful interpretation of the STATSGO database.

5.2 Classification

The classification algorithm appears to produce a useful division of the landscape. The resulting classes visually appear to be consistent in their ground type. Comparing a close up of the area around Roggen, Colorado with a Landsat scale classification image shows that specific classes are consistently related to specific ground types (fig. 5.1).

In order to examine the effect of the number of classes on the relationship between CENTURY and NDVI, a sensitivity study was performed. The classifier was parameterized to create between 5 and 50 classes in increments of 5. It was

still permitted to join classes together, but it would only do so if classes were extremely similar. The relationship between CENTURY and NDVI was then recomputed for each classification scheme.

Coefficients of correlation (R^2) were compared with the number of classes used to generate them. Figure 4.4 shows a plot of R^2, normalized by the number of points used in each regression, against the number of classes. Based on the T-Means test here is no significant difference between the R^2 values computed with greater then or equal to 20 classes and R^2 values computed with less than 20 classes. This indicates that the number of classes used when comparing CENTURY to NDVI is not very important. From analysis of the maps generated by this project, the number of classes used for each Landsat scene (from 5 to 15 classes, depending on the scene statistics) appears to be appropriate because dune crests and large sandy areas are clearly differentiated from interdune and other heavily vegetated areas.

5.3 Landsat Temporal Resolution

One of the greatest weaknesses of the present model could potentially be alleviated with higher temporal resolution satellite coverage. If the poor correlation between Landsat measurements of NDVI and CENTURY model output is purely due to random noise in the samples, then a greater number of samples may be the only way to improve the statistical correlation. For most of the scenes analyzed in this study only 3 years of imagery were available to correlate NDVI with CENTURY. In a temporal correlation, using three points to define a line leads to statistically poor correlations. For scene 33/32 (Northeastern Colorado) 8 dates were available and sufficiently cloud free to be analyzed. However, even 8 separate images did not generate a good correlation (Fig. 4.5). This may be due to other weaknesses in the model, or it may be that a very high temporal

resolution data set, such as is available from MODIS, would be necessary. It does indicate that doubling the number of Landsat images used from 3 to 6 is unlikely to substantially improve the results.

5.4 Landsat Spatial Resolution

Landsat spatial resolution appears necessary to accurately map sand dunes in the High Plains. The two other sensors that would allow higher temporal resolution NDVI imagery are MODIS and AVHRR. MODIS has a 250m pixel size, and AVHRR has a 1000m pixel size. Simple resampling results (figs 4.7 and 4.8) suggest that AVHRR data are largely useless for mapping sand dune reactivation, and that MODIS data are potentially very useful.

MODIS data can resolve most important features. It can not resolve individual dune crests in eastern Colorado, but dune crests tend to occur in close proximity, and the combination of Landsat data with MODIS data may prove adequate to study this area. Dunes in the Nebraska Sand Hills are readily resolved by MODIS, thus MODIS data is considered adequate to study these large linear dunes.

It is impossible to resolve important features such as the major linear dune crests in the Nebraska sand hills with AVHRR data. AVHRR would be an enormously useful resource because it has an extremely high temporal resolution and a long history. Because the dunes can not be resolved (fig. 4.8) it is impossible to determine how much signal is coming from dune crests and how much is coming from healthy vegetation in interdune areas. As a result there is no way of analyzing the vegetation on dune crests exclusively, even if Landsat data are used ahead of time to make an accurate map of the area.

5.5 Wind Speed

5.5.1 Single Index vs Temporal Integration

Wind measurements used in this study are meant to be an index of the general windfield across the High Plains, but wind varies substantially through time. Each point measurement used in this study contains a reasonably complete temporal sequence of hourly measurements. Ideally all of this data should be used and sand transport should be integrated under the time sequence of wind speed. Because it would also be necessary to generate a map of wind speed at each time step this process is not practical, so some approximation must be used.

Sand is dominantly transported by only the strongest winds, thus it makes sense to look at the average high wind speed for each location. I computed the mean monthly maximum wind speed as such an approximation. Other approximations might include looking at the top 2% cutoff, or incorporating the percent of time the wind stays above some threshold value. The top one and two percent cutoff values were analyzed and determined to be highly correlated with the mean monthly maximum (fig. 5.2), though the mean monthly maximum was always higher than either of these values. Because they are so well correlated it was determined not to be important which of these approximations was used and the original mean monthly maximum value was used.

Wind often changes seasonally, but the present single index should still be reasonable. Wind is often strongest in one or two months out of the year. The current index averages over all months. This is potentially a source of error, but because the index used is consistently above the threshold for sand transport it is assumed to be a small source of error. As long as wind speed is sufficiently high the amount of vegetation cover will dominate sand transport.

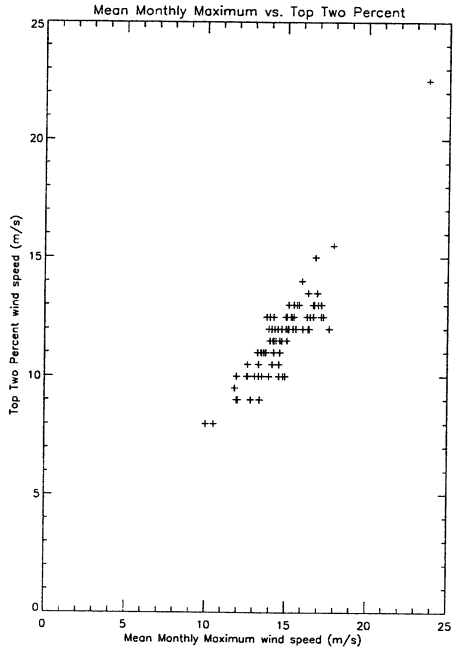

Figure 5.2: Comparison of Mean Monthly Maximum wind speed index to the top 2% of wind speeds

5.5.2 Sparse Spatial Distribution

This study required spatial wind maps; the only available data are point specific, thus we needed to spatially interpolate the existing data to create a map of the entire wind field. For each scene any wind values within 100km of the image boundary were collected and krigged to a 300m grid with IDL's Krig2D function. Despite the low resolution of the grid there was very little change from cell to cell, so 300m was deemed to be a high enough resolution for this study. In addition each point used appears to be highly correlated with its nearest neighbors thus the limited number of available points was not deemed to be a large source of error.

5.5.3 Homogeneity of Windfield

The number of data points available to generate a windmap are probably adequate because the resulting map is fairly homogenous (fig 5.3). If the data points available changed dramatically from one location to the next there would be reason to suspect that all of the variability was not captured in the current data collection. While it is still possible that this is the case, it appears likely that the wind field does indeed vary smoothly from wind station to wind station. In addition, the total variability across the High Plains appears to be low relative to the variability in vegetation cover. The mean monthly maximum wind speed in almost all cases is much higher than the threshold velocity for sand transport on bare soil, thus vegetation cover probably dominates the spatial variability and any lost variability in the wind field is probably small enough to be negligible for this study.

5.6 Sand Transport Equation

One disadvantage to this model is its reliance on a fieldplot-scale sand transport equation. This equation has limited accuracy and may not represent large scale reactivation properly. Effects such as differences in upwind fetch, sources of sediment, and downwind sinks which halt the migration of sand are not accounted for. Larger scale estimations, such as historical perspectives, implicitly account for such effects.

The sand transport equation used in this study comes from localized measurements of sand transport and may not be indicative of large scale sand dune reactivation. The sand transport equation comes from a study based on individual measurements of sand transport with respect to wind and vegetation cover on flat ground. Because these measurements do not explicitly account for larger

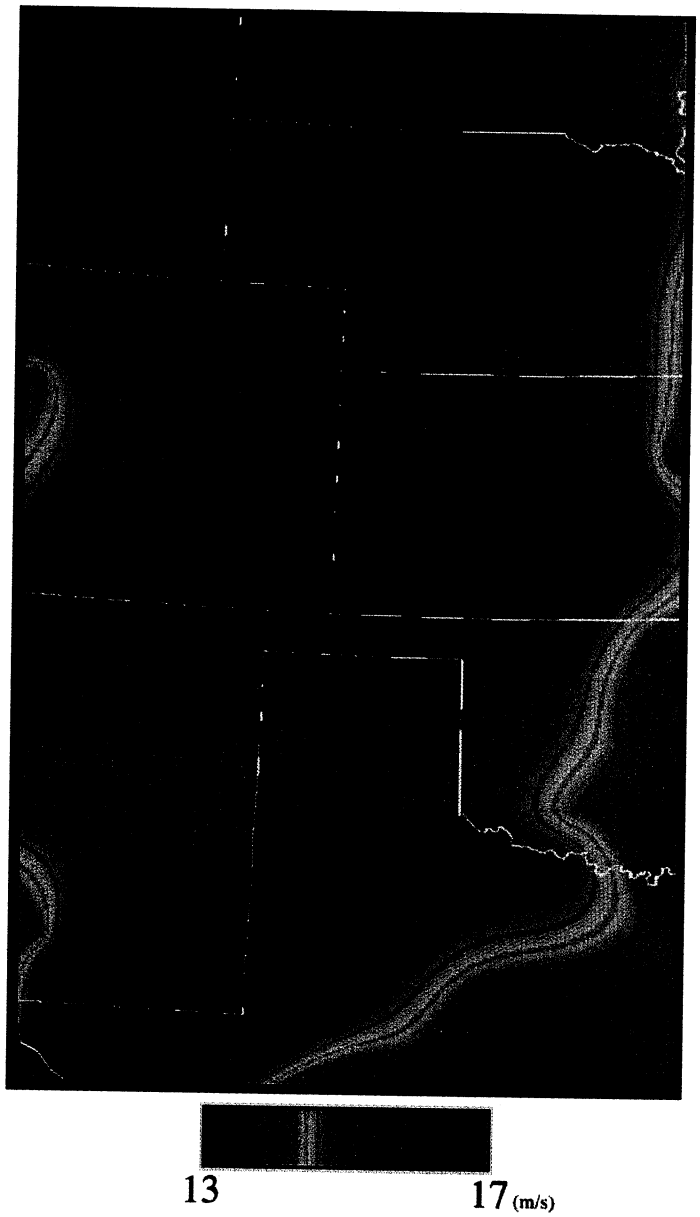

Figure 5.3: The Mean Monthly Maximum wind field across the High Plains exhibits only minor variability. Here black represents a wind speed of 13 m/s and dark red represents 17m/s as measured 10 meters above the ground, a total range of 4m/s. Contour lines represent approximately 0.15m/s increments.

scale terrain features it is unclear how well they will scale up to estimates of dune field activation. Upwind fetch and sediment sources/sinks are important variables in large scale reactivation not accounted for by small scale estimates. Bagnold (1941) and Shao et al. (1993) showed that sediment erodes much more readily when bombarded by sediment entrained upwind, especially fine grained sediment. In addition Van Boxel et al. (1999) showed that wind speed varies substantially at the surface of a dune due to speed up over the dune crest. Thus dune crests may actually activate at a slower regional wind speed due to higher localized wind speeds. Using a DEM it may be possible to include for this effect. Other studies have investigated larger scale dune reactivation, but cannot account for Landsat scale variability and thus are not useful for this study.

5.6.1 Limited Soil Information

This study has used only minimal soil parameterization. It may be possible to incorporate more detail from the STATSGO soils database. The sand transport equation developed by Bagnold (1941) allows for calculation of the threshold velocity on a bare sandy medium based on mean grain size. Beyond a simple mean grain size, the grain size distribution can be important in determining sand transport levels. Gillette and Chen (1999) showed that grain size distribution within a soil has a major impact on entrainment by wind. This is especially the case for dust transport, where the threshold velocity increases with decreasing grainsize. In this case larger grains will begin saltating at lower wind speeds and their impact can cause erosion of smaller grains which would have not have been eroded if the soil was only made up of small grains. At the moment the soil data available does not permit the inclusion of this detail, nor are there well developed sand transport equations that are a function of grain size distribution.

5.6.2 Proper Vegetative Measurements

It is impossible to make a single measurement of vegetation that describes all of the potential effects of vegetation on sand transport. Landsat measurements are used to estimate the percent of each pixel which is covered with vegetation, but this is not necessarily what is important in the estimation of sand transport. If within a single pixel twenty percent of the area is covered with a low standing, but dense, grass, large portions of that pixel may still be vulnerable to eolian erosion. However, if twenty percent of another pixel is covered with taller grasses and shrubs, those plants will have a substantial effect on windspeeds nearby and thus the remaining eighty percent of the pixel, though not covered by vegetation, will be less likely to experience substantial eolian erosion. Thus many studies of sand transport use a measure of vegetation described as the lateral cover. This measure incorporates the average height of vegetation as well as the areal coverage to provide a better estimate of the amount of vegetation that is actually blocking sand transport.

While it is impossible to measure vegetation height directly using Landsat data, it may be possible to estimate this by several other means. Different locations through out the High Plains can be characterized by different vegetation types. It may be possible to associate an efficiency factor with each area and multiply this by the percent cover as measured by Landsat to develop a better estimate of lateral cover. In addition a better spatial estimate of this efficiency factor may be possible by utilizing multi-angle data from the MISR sensor to estimate structural parameters, or by measuring the phenology of vegetation cover at a moderate resolution with the MODIS sensor to determine vegetation type at a moderate spatial resolution.

Chapter 6

Conclusions

6.1 Physics based modeling potential

This goal of this study was to develop and analyze a model for potential sand transport in the High Plains of North America. This study has illustrated an attempt to bring together the necessary components to run a simple, physics based model to estimate future sand transport across the High Plains. This study has shown that better modeling of future vegetation is a subject that needs substantial work, and has suggested several methods by which this modeling might be improved : a more detailed incorporation of the spatial variability in vegetation and soil type, higher temporal resolution satellite measurements and model estimates, and incorporation of recent rainfall data when estimating vegetation cover from NDVI. In addition, further improvements could be made to the model as a whole with a better understanding of the effects of vegetation on sand transport and by integrating sand transport over several years of wind data.

6.2 Spatial resolution

Landsat scale spatial resolution is required to study sand dunes in the High Plains. Small, localized dunefields such as those in Eastern Colorado effectively disappear with larger ($\geq$500m) pixel sizes. Dune crests may be the only areas that stand out. If these areas were averaged together with surrounding, vegetated

areas by low spatial resolution satellite imagery, the true instability of these dunes would not be captured. In addition it is not possible to map land use with enough accuracy using lower spatial resolution imagery because even large pivot irrigation systems are too small to detect. However, it may be possible to incorporate high temporal, low spatial resolution with the high spatial resolution data from Landsat to further improve the model.

6.3 Temporal Resolution

The benefit of increasing satellite temporal resolution is unclear. The simple test performed here showed no relationship between the number of images used and the correlation coefficient when regressing Century and NDVI values. It is possible that extremely high frequency imagery, such as bi-weekly MODIS data would be a substantial benefit to the model, but it is clear that simply collecting twice as many Landsat images does not substantially improve the results of the present model.

6.4 Areas of instability

This model has also mapped areas of potentially higher instability, though the present map is not suitable for planning purposes. At the moment careful interpretation of the output is required because of the poor correlation between NDVI and Century values. Some regions of apparent instability may only appear that way due to recent weather conditions or local soil color. It appears that the largest areas at risk are in the Nebraska Sand Hills, and portions of Eastern Colorado and Western Texas. Further areas at high risk are spread out across the High Plains and generally highly localized. This model does not map areas that are currently farmed, thus large areas may be at risk that are not shown in this model. In addition this model only maps areas of potential sand transport.

Dust, which has important implications for human health and well being, is not mapped by the present model.

6.5 Future Work

One of the major results of this thesis is the understanding of our current limitations in this field, and the suggestion of possible methods of improvement. There are many holes in our current understanding and in the available data that need to be filled before an accurate assessment of dune stability can be made. The area that needs the most work is the prediction of future vegetation cover. In addition, a better method of incorporating a time series of wind measurements and a denser network of weather stations would be beneficial.

The prediction of future vegetation could probably be improved with a more accurate model of vegetation response to climate, and a higher temporal resolution sequence of satellite and model estimates. One of the first improvements that needs to be investigated is the inclusion of high temporal resolution MODIS data. Though this would mean decreasing the spatial resolution of the model, but the increased ability to estimate the relationship between climate and vegetation would substantially out weigh this loss.

A better estimate of wind speed over time should be used. The current model only includes an index of windspeed. Winds may be highly seasonal in nature, so an estimate for each month should be used. Work needs to be done to determine the best wind index for this type of study, and what the effects of seasonal variation are.

Bibliography

Ahlbrandt, T., Swinehart, J., & Maroney, D. (1983). The dynamic Holocene dune fields of the Great Plains and Rocky Mountain basins, U.S.A. In M. Brookfield & T. Ahlbrandt (Eds.), Eolian Sediments and Processes (pp. 379–406). New York: Elsevier.

Armbrust, D. V. & Bilbro Jr., J. D. (1997). Relating plant canopy characteristics to soil transport capacity by wind. Agronomy Journal, 89, 157–162.

Asrar, G., Fuchs, M., Kanemasu, E., & Hatfield.J.L. (1984). Estimating absorbed photosynthetic radiation and leaf area index from spectral reflectance in wheat. Agron. J., 76, 300–306.

Bagnold, R. (1941). The Physics of Blown Sand and Desert Dunes. London: Methuen.

Barry, R. & Chorley, R. (1987). Atmosphere, Weather and Climate. New York: Methuen.

Buckley, R. (1987). The effect of sparse vegetation on the transport of sune sand by wind. Nature, 325, 426–428.

Buckley, R. (1998). Effects of vegetation on the transport of dune sand. Annals of Arid Zone, 35(3), 215–223.

Burke, I., Lauenroth, W., & Parton, W. (1997). Regional and temporal variation in net primary production and nitrogen mineralization in grasslands. Ecology, 78(5), 1330–1340.

Carlson, T., Perry, E., & Schmugge, T. (1990). Remote estimation of soil moisture availability and fractional vegetation cover for agricultural fields. Agric. For. Meteorol., 52, 45–69.

Carlson, T. N. & Ripley, D. A. (1997). On the relation between NDVI, fractional vegetation cover, and Leaf Area Index. Remote Sensing of the Environment, 62, 241–252.

Chavez, P. S. (1996). Image-based atmospheric corrections – revisited and improved. Photogrammetric Engineering & Remote Sensing, 62(9), 1025–1036.

EarthInfo (2000). National climatic data center summary of the day. Technical report, EarthInfo Inc., Boulder, CO.

Elmore, A., Mustart, J., Manning, S., & Lobell, D. (2000). Quantifying vegetation change in smei-arid environments: Precision and accuracy of spectral mixture analysis of the Normalized Difference Vegetation Index. Remote Sensing of the Environment, 73(1), 87–102.

Forman, S. & Maat, P. (1990). Stratigraphic evidence for late Quaternary dune activity near Hudson on the piedmont of northern Colorado. Geology, 18, 745–748.

Forman, S. L., Goetz, A. F., & Yuhas, R. H. (1992). Large-scale stabilized dunes on the High Plains of Colorado: Understanding the landscape response to Holocene climates with the aid of images from space. Geology, 20, 145–148.

Forman, S. L., Oglesby, R., Markgraf, V., & Stafford, T. (1995). Paleoclimatic significance of late Quaternary eolian deposition on the Piedmont and High Plains, central United States. Global and Planetary Change, 11, 35–55.

Forman, S. L., Oglesby, R., & Webb, R. S. (2001). Temporal and spatial patterns of Holocene dune activity on the Great Plains of North America: megadroughts and climate links. Global and Planetary Change, 29, 1–29.

Fryberger, S. & Dean, G. (1979). Dune forms and wind regime. In E. McKee (Ed.), A Study of Global Sand Seas, volume 1052 of U.S. Geological Survey Professional Paper.

Gillette, D. A. & Chen, W. (1999). Size distributions of saltating grains: and important variable in the production of suspended particles. Earth Surface Processes and Landforms, 24, 449–462.

Gillette, D. A. & Stockton, P. H. (1989). The effect of nonerodible particles on wind erosion of erodible surfaces. Journal of Geophysical Research, 94(D10), 12,885–12,893.

Gilmanov, T., Parton, W., & Ojima, D. (1997). Testing the 'century' ecosystem level model on data sets from eight grassland sites in the former ussr representing a wide climatic/soil gradient. Ecological Modelling, 96(1-3), 191–210.

Gregory, J., Mitchell, J., & Brady, A. (1997). Summer drought in the northern midlatitudes in a time-dependent CO_2 climate experiment. Journal of Climate, 10, 662–686.

Hagen, L. & Armbrust, D. (1994). Plant canopy effects on wind erosion saltation. Transactions of the ASAE, 37(2), 461–465.

Hansen, J., Fung, I., Lacis, A., Rund, D., Ruedy, R., & Russel, G. (1988). Global climate changes as forcast by Goddard Institute for Space Studies three dimensional model. Journal of Geophysical Research, 93, 9341–9364.

Holliday, V. (1989). Middle Holocene drought on the southern High Plains. Quaternary Research, 31, 74–82.

Holliday, V. (1995). Stratigraphic and paleoenvironments of the late Quaternary velly fills on the southern High Plains. Geological Society of America Memoir, 186, 136.

Huete, A., Jackson, R., & Post, D. (1985). Spectral response of a plant canopy with different soil backgrounds. Remote Sensing of the Environment, 17, 37–53.

Isaaks, E. H. & Srivastava, R. M. (1989). An Introduction to Applied Geostatistics. New York: Oxford University Press.

Lancaster, N. (1987). Development of linear dunes in the southwestern Kalahari. Journal of Arid Environments, 14, 233–244.

Lancaster, N. & Baas, A. (1998). Influence of vegetation cover on sand transport by wind: Field studies at Owens Lake, California. Earth Surface Processes and Landforms, 23, 69–82.

Lancaster, N. & Helm, P. (2000). A test of a climatic index of dune mobility using measurements from the southwestern United States. Earth Surface Processes and Landforms, 25, 197–207.

Landsat Project Science Office (cited 2002). Landsat 7 Science Data users Handbook. Greenbelt, Maryland: NASA.
`http://ltpwww.gsfc.nasa.gov/IAS/handbook/handbook_toc.html`

Loope, D., Swinehart, J., & Mason, J. (1995). Dune-dammed paleovalleys of the Nebraska Sand Hills: Intrinsic versus climatic controls on the accumulation of lake and marsh sediments. Geological Society of America Bulletin, 107, 396–406.

Madole, R. F. (1994). Stratigraphic evidenceof desertification in the west-central Great Plains within the past 1000 yr. Geology, 22(6), 483–486.

Manabe, S. & Wetherald, R. (1987). Large-scale changes in soil wetness induced by an increase in atmospheric carbon dioxide. Journal of the Atmospheric Sciences, 44, 1211–1235.

Metherell, A. (1992). Simulation of Soil Organic Matter Dynamics and Nutrient Cycling in Agroecosystems. PhD dissertation, Colorado State University.

Motavalli, P., Palm, C., Parton, W., Elliott, E., & Frey, S. (1994). Comparison of laboratory and modeling simulation methods for estimating soil carbon pools in tropical forest soils. Soil Biology & Biochemistry, 26(8), 935–944.

Muhs, D. & Maat, P. (1993). The potential response of eolian sands to greenhouse warming and precipitation reduction on the Great Plains of the U.S.A. Journal of Arid Environments, 25, 351–361.

Muhs, D. R. & Holliday, V. T. (1995). Evidence of active dune sand on the Great Plains in the 19th century from accounts of early explorers. Quaternary Research, 43, 198–208.

Muhs, D. R. & Holliday, V. T. (2001). Origin of late Quaternary dune fields on the Southern High Plains of Texas and New Mexico. Geological Society of America Bulletin, 113(1), 75–87.

Muhs, D. R., Stafford, T. W., Cowherd, S. D., Mahan, S. S., Kihl, R., Maat, P. B., Bush, C. A., & Nehring, J. (1996). Origin of late Quaternary dune fields of Northeastern Colorado. Geomorphology, 17, 129–149.

Muhs, D. R., Stafford Jr., T. W., Swinehart, J. B., Cowherd, S. D., Mahan, S. A., Bush, C. A., Madole, R. F., & Maat, P. B. (1997). Late Holocene eolian activity in the mineralogically mature Nebraska sand hills. Quaternary Research, 48, 162–176.

Muhs, D. R., Swinehart, J. B., Loope, D. B., Aleinikoff, J. N., & Been, J. (1999). 200,000 years of climate change recorded in eolian sediments of the High Plains of eastern Colorado and western Nebraska. In D. Lageson, A. Lester, & B. Trudgill (Eds.), Colorado and Adjacent Areas: Boulder, Colorado, Geological Society of America Field Guide 1.

Musick, H. B., Trujillo, S. M., & Truman, C. (1996). Wind-tunnel modelling of the influence of vegetation structure on saltation threshold. Earth Surface Processes and Landforms, 21, 589–605.

Nemani, R. & Running, S. (1989). Testing a theoretical climate-soil-leaf area hydrological equilibrium of forests using satellite data and ecosystem simulation. Agric. For. and Meteorol., 44, 245–260.

Oglesby, R. (1991). Springtime soil moisture, natural climatic variability, and North American drought as simulated by the NCAR community climate model. Journal of Climate, 4(9), 890–897.

Overpeck, Jonathan, T., Rind, D., & Goldberg, R. (1990). Climate-induced changes in forest disturbance and vegetation. Nature, 343(6253), 51–53.

Parton, W., Hartman, M., Ojima, D., & Schimel, D. (1998). Daycent and its land surface submodel: description and testing. Global and Planetary Change, 19(1-4), 35–48.

Parton, W., Schimel, D., & Cole, C. (1988). Dynamics of C, N, P, and S in grassland soils: A model. Biogeochemistry, 5, 109–131.

Parton, W., Scurlock, J., Ojima, D., Gilmanov, T., Scholes, R., Schimel, D., Kirchner, T., Menaut, J., Seastedt, T., Moya, E., Kamnalrut, A., & Kinyamario, J. (1993). Observations and modeling of biomass and soil organic-matter dynamics for the grassland biome worldwide. Global Biogeochemical Cycles, 7(4), 785–809.

Parton, W., Scurlock, J., Ojima, D., Schimel, D., & Hall, D. (1995). Impact if climate-change on grassland production and soil carbon worldwide. Global Change Biology, 1(1), 13–22.

Paruelo, J. & Lauenroth, W. (1996). Relative abundance of plant functional types in grasslands and shrublands of North America. Ecological Applications, 6(4), 1212–1224.

Pye, K. & Tsoar, H. (1990). Aelian sand and sand dunes. Boston, Massachusetts: Unwin Hyman.

Raupach, M., Gillette, D., & Leys, J. (1993). The effect of roughness elements on wind erosion threshold. Journal of Geophysical Research, 98(D2), 3023–3029. February 20th.

Rouse, J., R.H., H., Schell, J., Deering, D., & Harlan, J. (1974). Monitoring the vernal advancements and retrogradation (greenwave effect) of nature vegetation. Final report, NASA/GSFC, Greenbelt, MD.

Sala, O., Parton, W., Joyce, L., & Lauenroth, W. (1988). Primary production of the central grassland region of the United-States. Ecology, 69(1), 40–45.

Scambos, T. A., Dutkiewicz, M. J., Wilson, J. C., & Bindschadler, R. A. (1992). Application of image cross-correlation to the measurement of glacier velocity using satellite image data. Remote Sensing of the Environment, 42(3), 177–186.

Schlesinger, W., Fonteyn, P., & Reiners, W, A. (1989). Effects of overland-flow on plant water relations, erosion, and soil-water percolation on a Mojave Desert landscape. Soil Science Society of America Journal, 53(5), 1567–1572.

Shao, Y., Raupach, M., & Findlater, P. (1993). Effect of saltation bombardment on the entrainment of dust by wind. Journal of Geophysical Research, 98(D7), 12,719–12,726.

Spies, P.-J. & McEwan, I. K. (2000). Equilibrium of saltation. Earth Surface Processes and Landforms, 25, 437–453.

Stockton, P. H. & Gillette, D. A. (1990). Field measurement of the sheltering effect of vegetation on erodible land surfaces. Land Degredation & Rehabilitation, 2, 77–85.

Stokes, S. & Swinehart, J. (1997). Middle- and late-Holocene dune reactivation in the Nebraska Sand Hills, USA. The Holocene, 7, 263–272.

Tou, J. & Gonzalez, R. (1974). Pattern Recognition Principals. Reading, Massachusetts: Addison-Wesley.

Tucker, C. (1979). Red and photographic infrared linear combinations for monitoring vegetation. Remote Sensing of the Environment, 8, 127–150.

Van Boxel, J., Arens, S., & Van Dijk, P. (1999). Aeolian processes across transverse dunes. I: Modelling the air flow. Earth Surface Processes and Landforms, 24, 255–270.

Warner, A. S. (2000). Quantifying fractional ground cover on the climate sensitive High Plains using AVIRIS and Landsat TM data. Masters of Science, University of Colorado, Boulder, Geological Sciences Department.

Wasson, R. & Nanninga, P. (1986). Estimating wind transport of sand on vegetated surfaces. Earth Surface Processes and Landforms, 11, 505–514.

Wessman, C., Bateson, C., & Benning, T. (1997). Detecting fire and grazing patterns in tallgrass prairie using spectral mixture analysis. Ecological Application, 7(2), 493–511.

Wiggs, G. (1997). Sediment mobilisation by the wind (2nd ed.)., (pp. 357–372). London: Wiley. D.S.G. Thomas (Ed.).

Wiggs, G. F., Thomas, D. S., & Bullard, J. E. (1995). Dune mobility and vegetation cover in the Southwest Kalahari Desert. Earth Surface Processes and Landforms, 20, 515–529.

Wolfe, S. A. & Nickling, W. G. (1993). The protective role or sparse vegetation in wind erosion. Progress in Physical Geography, 17(1), 50–68.

Woodhouse, C. A. & Overpeck, J. T. (1998). 2000 years of drought variability in the central United States. Bulletin of the American Meteorological Society, 79(12), 2693–2714.